VOLUME 34 NUMBER 9

DEC 17 1929

THE PHYSICAL REVIEW

A JOURNAL OF EXPERIMENTAL AND THEORETICAL PHYSICS

CONDUCTED BY

THE

AMERICAN PHYSICAL SOCIETY

BOARD OF EDITORS

Managing Editor JOHN T. TATE, University of Minnesota, Minneapolis

G. BERTI, P. W. BRIDGMAN, L. W. MCKEEHAN, I. S. BOWEN, R. S. MULLIKEN, H. D. SMYTH, E. U. CONDON, C. J. DAVISSON, F. K. RICHTMYER

NOVEMBER 1, 1929

Precision Measurements in the K-Series of the Elements 48 Cd and 49 In. JOSEPH VALASEK 1021

Ranges of Ionizing Electrons in Helium - - - - - - - - THOMAS H. OSGOOD 1033

New Terms in the Oxygen Arc Spectrum - - - - - - - - RUDOLF PEERLEITER 1039

Relative Intensities of Nebular Lines - - - - - - - - JAMES H. BARTELMY, JR. 1047

On Methods of Filter Radiometry - - DONALD C. STOCKBARGER AND LAURENCE BURNS 1065

Packing of Homogeneous Spheres - - W. O. SMITH, PAUL D. FOOTE AND P. F. BUSANG 1271

Effect of Temperature Upon the Fluorescence of Some Organic Solutions - J. R. JOHNSON 1282

Letters to the Editor - - - - - - - - - - - - - - - - - - 1295

Book Reviews - 1301

PUBLISHED BY THE AMERICAN PHYSICAL SOCIETY

PUBLICATION OFFICE: 450A ...

THE AMERICAN PHYSICAL SOCIETY

OFFICERS OF THE SOCIETY

[illegible]	HENRY G. GALE	University of Chicago, Chicago, Ill.
[illegible] Presidents	W. F. G. SWANN	Bartol Research Foundation, Philadelphia, Pa.
[illegible]	W. L. SEVERINGHAUS	Columbia University, New York City
[illegible]	G. B. PEGRAM	Columbia University, New York City
[illegible]	JOHN T. TATE	University of Minnesota, Minneapolis, Minn.
[illegible] Secretary for [illegible] Pacific Coast	L. R. LEIB	University of California, Berkeley, Calif.

THE PHYSICAL REVIEW

Published by the American Physical Society at 450 Ahnaip St., Menasha, Wis. Executive office: University of Minnesota, Minneapolis, Minn. Two volumes annually, [illegible] issues per volume.

First series. From July 1, 1893, to January 1, 1913, the REVIEW was conducted by Edward L. Nichols, Ernest Merritt and Frederick Bedell, with the financial support of Cornell University. The first four volumes were issued annually; subsequent volumes, semi-annually; thirty-five volumes in all.

Second series. On January 1, 1913, the REVIEW was transferred to the American Physical Society as announced on the first page of the new series which was then begun. Since then it has been conducted by a Board of Editors elected by the Society. Semi-annual volumes begin in January and July. Since July 1, 1919, the REVIEW has been issued [illegible] a month.

Contributors are referred to page 2 of the advertisements for further information.

Annual Subscription, throughout the Postal Union, $10.00 in advance.

Single copies of current volume, $1.60.

General Index, 1893-1912, $4.00, in advance.

Back Volumes, $6.00 per volume; Back Numbers, $1.00 per copy for issues prior to July 1, 1919 (Vols. 1-13), $.60 per copy for issues subsequent thereto. Postage is free when remittance accompanies order; otherwise postage is extra. No bound volumes can be supplied. The REVIEW offers to purchase a limited number of First Series, Vol. 1, No. 1 ($2.00 each); Second Series, Vol. 7, No. 1, January 1916; Vol. 7, No. 2, February 1916; Vol. 7, No. 4, April 1916; and Vol. 7, No. 5, May 1916 (at $2.00 each).

Advertisements. Rates will be supplied by the Editor on request. Copy for each number must be received at Minneapolis two weeks prior to the date of issue; old copy is repeated until new copy is received. Send electrotypes direct to the printers, George Banta Publishing Co., Menasha, Wis.

A discount of ten percent is allowed subscription agencies and members of the American Physical Society.

Changes of address and Complaints of failure to receive the REVIEW, in the case of members of the Physical Society, should be addressed to the Treasurer; in the case of other subscribers to 450 Ahnaip St., Menasha, Wis.; or to the Editor. New copies can be sent free in response to complaint of non-delivery only if notice of non-delivery is received within three months of date of issue.

Editorial Correspondence should be addressed to the PHYSICAL REVIEW, University of Minnesota, Minneapolis, Minn.

Entered at the postoffice at Menasha, Wis., as second class matter.
Acceptance for mailing at special rate of postage provided for in section 1103, Act of October 3, 1917, authorized September 4, 1918.

Second Series *November 1, 1929* *Vol. 34, No. 9*

THE
PHYSICAL REVIEW

PRECISION MEASUREMENTS IN THE *K*-SERIES OF THE ELEMENTS 48 Cd AND 49 In

By Joseph Valasek
Department of Physics, University of Minnesota

(Received September 18, 1929)

Abstract

The wave-lengths of the α_2, α_1, β_3, β_1, and β_2 lines in the *K*-series of cadmium and indium were re-measured, using the precision spectrograph of Siegbahn and Larsson.

SINCE 1926 there has been in progress at Upsala a program of re-measurement of the wave-lengths of the principal spectrum lines in the short wave region of the *K* and *L*-series. These lines are being measured with greater precision by means of the new Siegbahn spectrometer. This paper is a continuation of the work. The instrument used, its adjustment, and the method of procedure have been explained in great detail by Larsson.[1]

The crystal used was one of the so-called "precision calcites" (designated as P.K.2). This crystal has an unworked cleavage surface of 14 by 24 mm. Reflections off different parts of the crystal plate, 6 mm apart, were found to agree within one second of arc. In spite of this, however, the values given here are based on pairs of exposures in which the reflecting areas were not farther apart than 0.6 mm. The widths of the spectrum lines were not much greater than the width of the slit used which was 0.03 mm, the $\beta_{1,3}$ doublet being easily resolved, (separation 0.066 mm). The cadmium spectrograms were taken with a camera length of 406.19 mm except for three plates (Nos. 1, 2, 8) taken with a camera length of 622.11 mm. The indium spectrograms were all taken with the longer camera.

The glancing angles, ϕ, of the lines α_2, α_1, and β_1 of In and Cd, and β_3 of In, were measured by the Siegbahn displacement method[1] in which

$$2\phi = 2\phi_0 + 2\Delta\phi, \text{ where } 2\Delta\phi = (a/r).$$

$2\phi_0$ is 180° less the angle of rotation of the crystal between the two exposures, a is the small distance between the two lines on the photographic plate and r is the distance from slit to plate. The distances between lines on the plate were measured on a Gaertner comparator by taking 30 to 60 settings on each line in sets of ten using different parts of the screw. The distances

[1] Larsson, Phil. Mag. (7) **3**, 1136 (1927).

r had been measured by the method described by Larsson. The angle ϕ is reduced to 18°C by the formula:

$$d\phi = 2.15(T - 18) \tan \phi,$$

which gives the correction to ϕ in seconds of arc. The formula is based on an expansion coefficient of 1.04×10^{-5} perpendicular to the reflecting planes. To make this correction the temperature of the crystal was measured to

TABLE I.

Plate	Elem.	Line	$2\phi_0$	a mm	$2\Delta\phi$	T°C	ϕ	λX.U.
V_1	Cd	$K\alpha_1$	10° 9′ 50.9″	0.5651	3′ 7.4″	18.2	5° 3′ 21.8″	533.901
2	"	"	10 4 52.5	0.3380	1 52.1	17.9	5 3 22.3	533.915
8	"	"	10 4 54.5	0.3308	1 49.6	18.3	5 3 22.1	533.911
45	"	"	10 4 53.7	0.2154	1 49.3	18.7	5 3 21.6	533.895
46	"	"	10 4 58.0	0.2061	1 44.4	19.7	5 3 21.5	533.892
47	"	"	9 59 58.9	0.7966	6 44.6	20.1	5 3 22.1	533.910
						Average	5 3 21.9	533.904
3	In	$K\alpha_1$	9 35 8.2	1.0093	5 34.6	17.5	4 50 21.3	511.064
4	"	"	9 35 2.5	1.0268	5 40.4	19.5	4 50 21.7	511.075
5	"	"	9 39 38.2	0.1911	1 3.4	18.7	4 50 20.9	511.051
10	"	"	9 40 8.1	0.1058	0 35.1	17.1	4 50 21.5	511.067
						Average	4 50 21.4	511.064
2	Cd	$K\alpha_2$	10 4 52.5	1.2494	6 54.3	17.9	5 5 53.4	538.336
45	"	"	10 4 53.7	0.8069	6 49.8	18.7	5 5 51.8	538.290
47	"	"	9 59 58.9	1.3912	11 46.5	20.1	5 5 53.1	538.326
						Average	5 5 52.8	538.317
3	In	$K\alpha_2$	9 35 8.2	1.9210	10 36.9	17.5	4 52 52.5	515.486
4	"	"	9 35 2.5	1.9414	10 43.5	19.5	4 52 52.7	515.492
5	"	"	9 39 38.2	1.1041	6 6.1	18.7	4 52 52.3	515.480
10	"	"	9 40 8.2	1.0150	5 36.5	17.1	4 52 52.2	515.478
						Average	4 52 52.4	515.484
48	Cd	$K\beta_1$	8 54 57.7	0.4273	3 37.0	18.2	4 29 17.2	474.060
49	"	"	8 54 31.4	0.4833	4 5.4	17.5	4 29 18.3	474.091
50	"	"	8 54 54.2	0.4384	3 42.6	16.7	4 29 18.2	474.088
						Average	4 29 17.9	474.080
6	In	$K\beta_1$	8 30 6.7	0.9313	5 8.8	19.8	4 17 38.1	453.586
7	"	"	8 34 22.3	0.1578	0 52.3	18.6	4 17 37.4	453.566
9	"	"	8 34 14.8	0.1812	1 0.5	19.1	4 17 37.8	453.578
						Average	4 17 37.8	453.577
6	In	$K\beta_3$	8 30 6.7	1.0621	5 52.2	19.8	4 17 59.8	454.221
7	"	"	8 34 22.3	0.2931	1 37.2	18.6	4 17 59.9	454.223
						Average	4 17 59.9	454.222

0.1°C by means of a thermometer inserted into the holder of the crystal. Readings were taken regularly during each exposure. The wave-lengths were calculated by the Bragg formula:

$$\lambda = 2d \sin \phi,$$

the first order being used throughout. The value of d was assumed to be:

$$d = 3029.040 \text{ X.U. or } \log 2d = 3.782\ 3350.$$

The Rydberg frequencies were calculated using $\log R = 5.040\ 3531$.

The potential across the x-ray tube was, on the average, 50 kv, and the current was about 3 m.a. The indium metal was rubbed into fine cuts on the copper target. The cadmium was a thin plate dove-tailed into the face of the target. Exposures of one to five hours were required.

Table I gives the results obtained by the Siegbahn displacement method. Table II contains a summary of these results calculated into Rydberg frequencies. Leide's recent values for the wave-lengths[2] are given in column four for comparison. These results had been obtained using one of Siegbahn's earlier spectrographs. The disagreement in the wave-lengths of β_1 is largely due to the fact that Leide was unable to resolve the doublet.

TABLE II.

Elem.	Line	λ	λ Leide	ν/R	$(\nu/R)^{1/2}$
Cd	$K\alpha_1$	533.904	533.86	1706.804	41.3135
Cd	$K\alpha_2$	538.317	538.29	1692.809	41.1438
Cd	$K\beta_1$	474.080	474.29	1922.185	43.8427
In	$K\alpha_1$	511.064	511.03	1783.083	42.2266
In	$K\alpha_2$	515.484	515.46	1767.794	42.0451
In	$K\beta_1$	453.577	453.72	2009.074	44.8227

Table III contains the results of measurements of the β_2 and β_3 lines relative to β_1. The third column (n) gives the number of plates which were measured and averaged to obtain the value of $\Delta\phi$. The results were reduced by means of the differential form of Bragg's formula: $\Delta\lambda = 2d \cos\phi\Delta\phi$.

TABLE III. *Wave-lengths relative to* β_1.

Elem.	Line	n	$\Delta\phi$	$\Delta\lambda$	λ	λ Leide	ν/R	$(\nu/R)^{1/2}$
Cd	$K\beta_2$	(2)	5′ 37.3″	9.877	464.203	464.39	1963.085	44.3067
Cd	$K\beta_3$	(2)	0 21.6	0.632	474.712	—	1919.627	43.8136
In	$K\beta_2$	(2)	5 24.4	9.501	444.076	444.08	2051.680	45.2955
In	$K\beta_3$	(5)	0 22.5	0.657	454.234	—	2006.168	44.7903

The above measurements were all made in the Physical Laboratory of the University of Upsala. The writer takes this opportunity to express his thanks to Professor Siegbahn for the many courtesies shown him during his stay at that institution.

[2] Leide, Diss. Lund 1925; Zeits. f. Physik **39**, 686 (1926).

THE RANGES OF IONIZING ELECTRONS IN HELIUM

By Thomas H. Osgood
Department of Physics, University of Pittsburgh

(Received September 19, 1929)

Abstract

The paper shows that a fourth power law for the absorption of ionizing electrons in helium represents experimental results only for initial energies greater than 250 electron volts. For initial energies less than 200 electron volts, the formula

$$x=(a/c^3)[cE-f+f\log(cE-f)]$$

is deduced, where x is the range of an electron of initial energy E electron volts, and the remaining quantities are constants. The formula is in agreement with the available experimental evidence, and appears to be applicable, with suitable changes in the constants, to other gases.

INVESTIGATIONS of the behavior of ionizing electrons in passing through gases are concerned with three interdependent quantities; the initial energy of the electrons, the distance which they travel and the number of ions they produce. Most workers[1] have endeavoured to find relationships between the energy of an electron and the average number of ions produced by it per unit distance travelled; a few,[2] in more recent years, have found the total number of ions in the whole distance travelled as a function of the initial energy of the electron, and have made some direct measurements of the ranges of the particles. It is necessary to distinguish between what, in this paper, is called the range of a particle and its track-length. The former is taken to mean the straight line distance from its origin to the point at which it ceases to ionize; the latter denotes the distance travelled by the electron measured along the actual path, as can be done for beta particles in a cloud expansion photograph.

To represent the absorption of cathode rays by matter, J. J. Thomson formulated the fourth power law, which has been verified experimentally by Whiddington,[3] C. T. R. Wilson,[4] Nuttall and Williams[5] and others. This law is concerned with the track-length, not with the range of the particles. Electrons with small initial energy, below about 2500 electron volts, cannot be studied adequately by cloud expansion methods, for they produce only

[1] For example: W. Kossel, Ann. d. Physik **37**, 393 (1912); S. Bloch, Ann. d. Physik **38**, 559 (1912); F. Mayer, Ann. d. Physik **45**, 1 (1914); Hughes and Klein, Phys. Rev. **23**, 450 (1924); K. T. Compton and Van Voorhis, Phys. Rev. **26**, 436 (1925).

[2] Johnson, Phys. Rev. **10**, 609 (1917); Anslow, Phys. Rev. **25**, 484 (1925); Lehmann and Osgood, Proc. Roy. Soc. **A115**, 609 (1927); Lehmann, Proc. Roy. Soc. **A115**, 624 (1927).

[3] Whiddington, Proc. Roy. Soc. **A86**, 360 (1912).

[4] C. T. R. Wilson, Proc. Roy. Soc. **A104**, 1 (1923).

[5] Nuttall and Williams, Phil. Mag. **2**, 1109 (1926).

the "sphere" tracks described by C. T. R. Wilson. Electrical methods, with gas at low pressures must therefore be used for their investigation. It is the purpose of this paper to deduce from the experimental evidence now available, relationships between the initial energies and the ranges in helium of ionizing electrons which cannot be studied by cloud expansion photographs.

Purely electrical experiments devised to measure the number of ions produced per unit distance in a gas by moving electrons determine the ionization along the range (as defined above), not along the track. The faster the electron moves, however, the more nearly the ionization per unit distance along the range approaches the same quantity per unit distance along the track, since fast electrons suffer comparatively infrequent abrupt deviations from their original direction. The ionization per unit distance along the range is, of course, greater than the ionization per unit distance along the track.

Since in a stream of moving electrons no individual particle pursues exactly the same track as its neighbour, the quantities with which we are concerned are the average values for a large number. It is possible to produce a beam of electrons whose initial energies differ by only a few percent.[6] With these restrictions, let E be the initial energy of a moving electron, measured in electron volts, n the total number of ions which it makes before ceasing to ionize, and x its range. Then dn/dx represents the ionization per unit distance along the range. Experiments by Lehmann[2] have shown that for values of E between 190 and 1060 volts there exists a linear relation between E and n; that is

$$n = aE + b \tag{1}$$

where a and b are constants. There is good reason for believing that this equation is true also for all high-speed beta particles. The fourth power law, which may be expressed as

$$\frac{1}{4}\frac{m^2v^4}{e^2} = E^2 = \frac{NR}{K} \qquad \text{(Nuttall and Williams)}$$

where N is the atomic number of the absorbing gas, K is a constant, R the track length of the electron, v its velocity and e and m its charge and mass, has been shown above not to be strictly applicable unless the track length can be measured, yet it should be at least an approximation to the truth if we write

$$E^2 = kx. \tag{2}$$

Here x is the range of the electron and k another constant. Eqs. (1) and (2) can be combined, for

$$dn/dx = a(dE/dx) \tag{1a}$$

and

$$2E(dE/dx) = k. \qquad \text{That is}$$

$$dn/dx = (ka)/2E. \tag{3}$$

[6] Lehmann and Osgood, Proc. Camb. Phil. Soc. **22**, 731 (1925), and Ref. 2.

If dn/dx be plotted as a function of $(1/E)$, the resulting graph should be a straight line, passing through the origin. This linear relation was shown to be true for high-speed cathode rays in air many years ago.[7]

Bearing this in mind, it seemed worth while to plot values of dn/dx as a function of $1/E$ for slower moving electrons. The most reliable experimental values of dn/dx are those of K. T. Compton and Van Voorhis[1] as corrected by their critique[8] of June, 1926. They expressed their results as a graph in which the ionization per unit distance along the range was shown as a function of E, over the range 25–300 volts. In Fig. 1, which deals with helium at 1 mm pressure, values of dn/dx are plotted as ordinates and those of $1/E$ as abscissas; Fig. 2 shows, on a different scale, part of the same curve

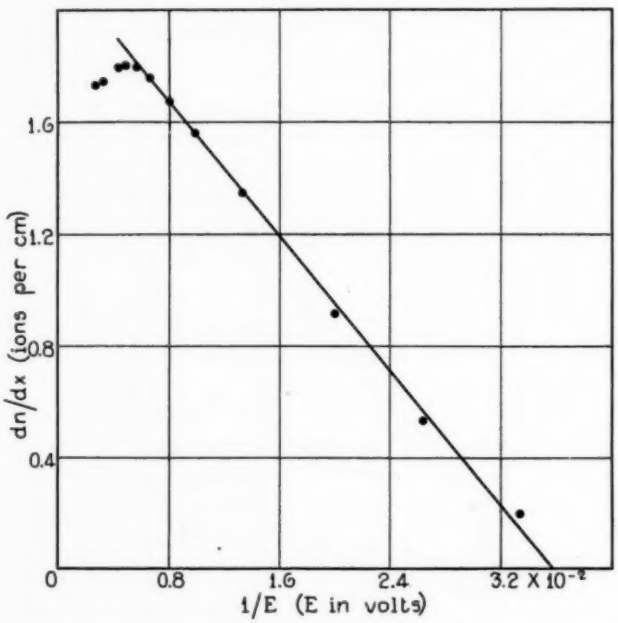

Fig. 1. Showing the relation between the ionization produced by an electron per unit distance along its range (dn/dx) and the reciprocal of its initial energy ($1/E$) measured in electron volts; based on the experimental results of K. T. Compton and Van Voorhis.

amplified by a few points from the work of Kossel, Glasson and Durack on high-speed electrons. These were obtained experimentally for air, but have been reduced to a helium standard by assuming from the mass absorption law that this gas is seven times as transparent as air. Fig. 2 also shows, as a full line, a plot of Eq. (3) using the constant for the fourth power law as given by Nuttall and Williams. The following interesting features are apparent: (*a*) For initial energies greater than 250 electron volts, the ranges of electrons are approximately representable by a fourth power law (dotted line, Fig. 2), the constant, as is to be expected, differing from that given by

[7] See S. Bloch, Ref. 2.

[8] K. T. Compton and Van Voorhis, Phys. Rev. **27**, 724 (1926)

Nuttall and Williams; (*b*) for energies less than 200 electron volts, a fourth power law is quite inadequate to represent the experimental results; (*c*) from 30 to 200 electron volts, the relation between dn/dx and $1/E$ is linear (Fig.1); (*d*) the transition between the two types of absorption is sharp, covering approximately the range 200–250 electron volts.

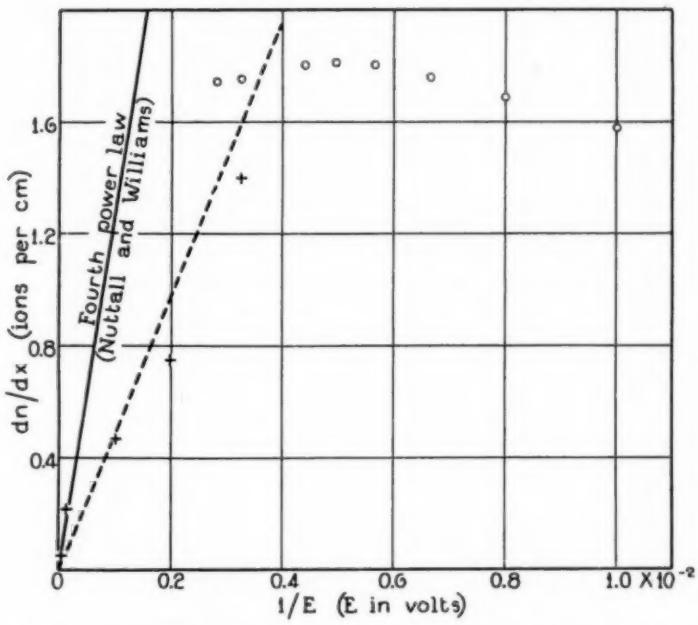

Fig 2. Showing part of the curve of Fig. 1 amplified by results from the work of Kossel, Glasson and Durack.

The observation (*c*) can be used to find a formula for the ranges of electrons between the limits specified, provided Eq. (1) is also true between these limits. This was experimentally proved by Johnson.[2] The equation to the straight line in Fig. 1 may be written

$$dn/dx = c - f/E,$$

where c and f are constants. Combining this with Eq. (1a),

$$dx = [(aE)/(cE - f)]dE,$$

which integrates to

$$x + h = (a/c^2)[cE - f + f \log (cE - f)], \tag{4}$$

where h is a constant of integration. This is small, and may for the present be neglected, since the straight line in Fig. 1 cuts the horizontal axis very near the point corresponding to the ionization potential of helium. The values of the constants are $a = 0.0328$ per volt, $c = 2.17$ per cm, $f = 61.5$ volts per cm. The value of a has been taken by extrapolating a curve given

by Lehmann, which was obtained under more reliable conditions than Johnson's. Putting $h=0$, the Eq. (4) is represented graphically in Fig. 3.

Since the formula (4) is based directly on experimental evidence, there is no reason to doubt its validity. It would be interesting, however, to check it by comparison with actual measurements of the ranges of electrons, as this would test the consistency of the experimental observations obtained by different methods. The available data are scanty. The value of x for

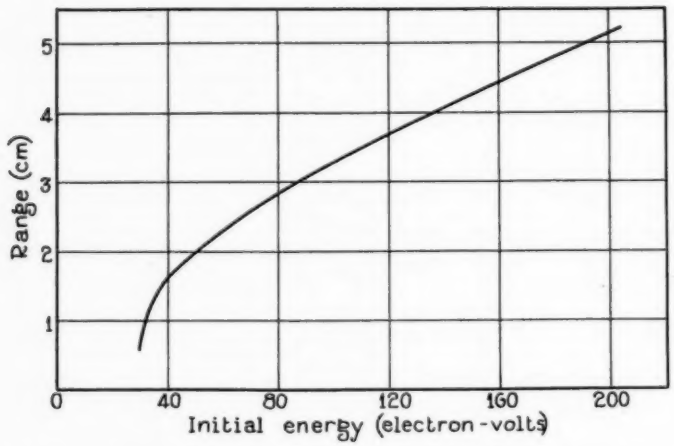

Fig. 3. Graph of Eq. (4) showing the ranges of electrons in helium at 1 mm pressure, as a function of their initial energy.

$E=190$ electron volts agrees well with the result obtained by Lehmann.[9] The curves given by Johnson are not definite enough to provide a comparison.

K. T. Compton and Van Voorhis have given results for many gases. The general trend of their curves is the same for all, including helium, and hence the conclusions arrived at in this paper are applicable, with suitable changes in the constants, to other gases.

Experiments are in progress in this laboratory to verify Eq. (1) for slow moving ionizing electrons, and to find their ranges by direct measurement.

[9] Lehmann, Ref. 2, p. 625, Fig. 1.

NEW TERMS IN THE OXYGEN ARC SPECTRUM

By Rudolf Frerichs*
University of Michigan, Ann Arbor

(Received September 27, 1929)

Abstract

Methods have been developed for the powerful excitation of the oxygen arc spectrum in the absence of bands, in large diameter heavy current discharge tubes and in narrow capillary quartz discharge tubes. In both tubes the green auroral line appears strongly. The oxygen arc spectrum has been photographed with these discharge tubes with large dispersion and many new lines have been observed. Fifty new lines have been classified in the oxygen arc spectrum involving six new triplet terms and one new singlet term based on the $2s^22p^3(^2D)$ and $2s^22p^3(^2P)$ configurations of the ion.

Apparatus and Procedure

THE strong excitation of the oxygen arc spectrum in discharge tubes is often rendered difficult by the appearance of numerous bands of the neutral and ionized molecule. These bands may be easily eliminated in two ways. One method is similar to the well-known experiments of Wood[1] on the excitation of the Balmer spectrum in absence of hydrogen bands. The atoms formed in the oxygen discharge show a strong tendency to recombine under the influence of any catalytically acting substance. With current densities of as little as 50 milliamperes/cm² the walls of the tube are strongly heated, the sodium of the glass vaporizes and accelerates catalytically the recombination of the atom with the emission of the oxygen band spectrum. The recombination may be prevented by water-cooling the glass walls and part of the measures here described were made with such water-cooled discharge tubes. The tubes had a length of about 60 centimeters and diameters of 30 to 50 millimeters. Large double-walled brass electrodes, cooled by flowing water, were set in side-tubes so that the discharge could be observed end-on. A constant current of 5 amperes from a 10 kw 2000 volt generator was sent through the tubes, and regulated by suitable ballast resistances. Oxygen either electrolytic or obtained by heating potassium permanganate was purified by liquefaction, dried, and drawn constantly through the discharge tube by an oil pump. At a pressure of a few millimeters the discharge formed a rosy core along the axis of the tube and under these conditions the oxygen arc spectrum is very brilliant and the green aurora line 5577.350A appears strongly. Slight impurities on the glass tube wall greatly diminish the intensity of the arc lines. Dust or sealing wax particles have a catalytic action on the recombination of the atoms into molecules. Dusting the walls with salts like alkali chlorides, which have no affinity for

* International Education Board Fellow.
[1] R. W. Wood, Proc. Roy. Soc. London **A97**, 455 (1920).

oxygen, however suppresses the recombination strongly. With such discharge tubes, the oxygen arc spectrum was photographed with large glass and quartz spectrographs built in this laboratory.

The oxygen arc spectrum may also be brilliantly excited by the use of high current densities in narrow capillaries. Oval quartz capillaries of 1×2 milli-

TABLE I.

Intensity	Wave-lengths	Wave-numbers (vacuum)	Classification	Wave-numbers (calculated)
5	8819.60	11335.27		
2	8586.00	11643.67		
1	8575.32	11658.18		
1	8508.66	11749.51		
1	8429.128	11860.37	$3s(^3P):{}^3P_0-4p(^3D):{}^3D_1$	11860.27
2	8428.342	11861.47	$3s(^3P):{}^3P_1-4p(^3D):{}^3D_2$	11861.49
4	8426.326	11864.46	$3s(^3P):{}^3P_2-4p(^3D):{}^3D_3$	11864.46
1	8424.780	11866.49	$3s(^3P):{}^3P_1-4p(^3D):{}^3D_1$	11866.58
1	8420.968	11871.87	$3s(^3P):{}^3P_2-4p(^3D):{}^3D_2$	11871.85
4	8235.408	12139.38	$3s(^3D):{}^3D_1-3p(^3D):{}^3P_2$	12139.45
15	8233.085	12142.80	$3s(^3D):{}^3D_1-3p(^3D):{}^3P_{1,0}$	12142.85
10	8230.016	12147.32	$3s(^3D):{}^3D_2-3p(^3D):{}^3P_2$	12147.32
10	8227.680	12150.77	$3s(^3D):{}^3D_2-3p(^3D):{}^3P_{1,0}$	12150.72
20	8221.829	12159.40	$3s(^3D):{}^3D_3-3p(^3D):{}^3P_2$	12159.34
4	7995.086	12504.25	$3p(^4S):{}^3P_2-3s(^3D):{}^3D_3$	12504.25
1	7987.404	12516.26	$3p(^4S):{}^3P_2-3s(^3D):{}^3D_2$	12516.27
2	7987.036	12516.84	$3p(^4S):{}^3P_{1,0}-3s(^3D):{}^3D_2$	12516.83
1	7982.408	12524.10	$3p(^4S):{}^3P_2-3s(^3D):{}^3D_1$	12524.14
1	7981.990	12424.75	$3p(^4S):{}^3P_{1,0}-3s(^3D):{}^3D_1$	12524.70
4	7952.182	12571.72	$3s(^3D):{}^3D_1-3p(^3D):{}^3F_2$	12571.72
6	7950.824	12573.87	$3s(^3D):{}^3D_2-3p(^3D):{}^3F_3$	12573.91
10	7947.566	12579.00	$3s(^3D):{}^3D_3-3p(^3D):{}^3F_4$	12579.00
3	7947.204	12579.59	$3s(^3D):{}^3D_2-3p(^3D):{}^3F_2$	12579.59
3	7943.178	12585.96	$3s(^3D):{}^3D_3-3p(^3D):{}^3F_3$	12585.96
3	7480.652	13364.15	$3s(^3P):{}^3P_0-3p(^3P):{}^3D_1$	13364.05
3	7479.148	13366.84	$3s(^3P):{}^3P_1-3p(^3P):{}^3D_2$	13366.95
2	7477.264	13370.22	$3s(^3P):{}^3P_1-3p(^3P):{}^3D_1$	13370.36
5	7476.473	13371.65	$3s(^3P):{}^3P_2-3p(^3P):{}^3D_3$	13371.65
2	7473.226	13377.47	$3s(^3P):{}^3P_2-3p(^3P):{}^3D_2$	13377.31
2	7471.374	13380.75	$3s(^3P):{}^3P_2-3p(^3P):{}^3D_1$	13380.72
5	7157.360	13967.80	$3d(^4S):{}^3D_{1,2}-3p(^3D):{}^1P_1$	13970.2
1	6727.138	14861.06	$3s(^4S):{}^5S_2-3p(^4S):{}^3P_{0,1}$	14861.28
5	6727.866	14861.68	$3s(^4S):{}^5S_2-3p(^4S):{}^3P_2$	14861.84
4	6654.121	15024.14		
5	6374.292	15683.64		
4	6366.282	15703.42		
3	6324.682	15806.71	$3d(^4S):{}^3D_{1,2,3}-3p(^3D):{}^3P_2$	15806.43
1	6323.283	15810.21	$3d(^4S):{}^3D_{1,2}-3p(^3D):{}^3P_{1,0}$	15809.83
1	6266.692	15952.98		
2	6264.346	15958.95	7.73	
5	6261.314	15966.68		
1	6258.965	15972.67	11.99	
3	6256.616	15978.67		
3	6106.398	16371.76		
3	5995.198	16675.43		
1	5993.102	16681.24		
2	5991.852	16684.72		
1	5991.255	16686.39		
5	5750.424	17385.22	58.61	
3	5731.103	17443.83		
1	5720.613	17475.81	31.98	
3	5410.76	18476.6	7.4	(wave-lengths by Fowler: Report on line spectra)
4	5408.59	18484.0		
3	5404.87	18496.7	12.7	

TABLE I. (*Continued*)

Intensity	Wave-lengths	Wave-numbers (vacuum)	Classification	Wave-numbers (calculated)
5	4233.32	23615.5	} 58.9	} wave-lengths by Fowler: Report on line spectra
3	4222.78	23674.4		
2	4217.09	23706.4	} 32.0	
10	3954.387	25279.36	$3p(^4S):{}^3P_2-3s(^2P):{}^3P_2$	25279.34
5	3954.596	25279.87	$3p(^4S):{}^3P_{1,0}-3s(^2P):{}^3P_2$	25279.87
2	3953.056	25289.73	$3p(^4S):{}^3P_2-3s(^2P):{}^3P_1$	25289.70
1	3952.982	25290.24	$3p(^4S):{}^3P_{1,0}-3s(^2P):{}^3P_1$	25290.26
3	3951.987	25296.57	$3p(^4S):{}^3P_{1,0}-3s(^2P):{}^3P_0$	25296.57
1	3825.530	26132.78	$3s(^2D):{}^3D_1-3p(^2P):{}^3D_2$	26132.51
4	3825.249	26134.70	$3s(^2D):{}^3D_2-3p(^2P):{}^3D_3$	26134.72
3	3825.090	26135.65	$3s(^2D):{}^3D_2-3p(^2P):{}^3D_1$	26135.92
3	3824.425	26140.33	$3s(^2D):{}^3D_1-3p(^2P):{}^3D_2$	26140.38
—	—	—	$3s(^2D):{}^3D_2-3p(^2P):{}^3D_1$	26143.79
10	3823.469	26146.85	$3s(^2D):{}^3D_3-3p(^2P):{}^3D_3$	26146.74
—	—	—	$3s(^2D):{}^3D_3-3p(^2P):{}^3D_2$	26152.40
—	2883.82	34666.3	$3s(^4S):{}^3S_1-3p(^2D):{}^1P_1$	34663.5
				(wave-lengths by Hopfield l.c. (λvac.!))
—	1217.6	82128.78	$2p:{}^1S_0-3s(^2P):{}^1P_1$?	—
—	1152.0	86805.86	$2p:{}^1D_2-3s(^2P):{}^1P_2$?	
—	999.47	100053.0	$2p:{}^1D_2-3s(^2P):{}^1P_1$?	
—	990.73[2]	100935.7	$2p:{}^3P_0-3s(^2D):{}^3D_1$	100922
—	990.11	100998.9	$2p:{}^3P_1-3s(^2D):{}^3D_{1,2}$	100981 100989
—	988.67	101146.0	$2p:{}^3P_2-3s(^2D):{}^3D_{1,2,3}$	101128 101140 101148

meters cross-section were used, with heavy iron electrodes in side tubes, externally water-cooled. These tubes carried steady currents of 1.2 to 1.5 amperes. Spectrograms were made with the 6.5 meter grating in Paschen mounting in the third basement of the laboratory. The temperature was so constant here that exposures of 72 hours showed no broadening of the lines. As an indication of the intensity of the light source it may be said that the strong infra-red doublet λ8446A of oxygen was strongly recorded in the first order of the grating on neocyanin plates in 10 seconds. Spectrograms were made on Eastman neocyanin and kryptocyanin plates, Ilford panchromatic plates and Cramer contrast plates. The iron arc lines were used as standards. Part of the exposures were made with commercial oxygen and showed weakly the strongest nitrogen lines as well as argon lines which were also used as standards.

In contrast to other observers[3] who found the auroral line 5577.350A only in wide tubes, it appeared likewise strongly in the narrow capillaries and was photographed with the grating. It is possible that the slight argon content of the oxygen used may have strengthened the line. Such powerful

[2] Unpublished classification of S. B. Ingram, privately communicated.

[3] J. C. McLennan, J. H. McLeqd and W. C. McQuarrie, Proc. Roy. Soc. London **A114**, 1 (1927).

excitation of the auroral line in narrow capillaries would greatly simplify investigations of the Zeeman effect of this line in comparison with the methods hitherto[4] used.

Table I contains the lines measured on the spectrograms taken with the big grating. It is noteworthy that none of the oxygen spark lines in the visible or near ultra-violet appear in direct current discharges in oxygen. The lines 2883 and 3954 previously given as spark lines[5] belong to the arc spectrum. The latter is not identical with a spark-line of the same wave-length, since this line belongs to a spark doublet whose other component does not appear in the oxygen arc spectrum.

In Table I there are, among other lines, all the unclassified lines observed by Runge and Paschen.[6] Our exposures with the grating extend only to 3800A and we have not observed the region of the short wave-length lines measured by Schniederjost[7] and Jevons.[8] Jevons has however shown that all

TABLE II.

	$2p$	$^3P_2$:109831 $^3P_1$:109672 $^3P_0$:109605	$^1D_2$, $^1S_0$		
		$2s^22p^3$:^4S	$2s^22p^3$:^2D	$2s^22p^3$:^2P	$2s2p^4$:^4P
	$3s$	$^5S_2$:36069.0 $^3S_1$:33043.3	$^3D_3$: 8702.91 $^3D_2$: 8690.89 $^3D_1$: 8683.02 $^1D_2$	$^3P_2$: − 4072.10 $^3P_1$: − 4082.54 $^3P_0$: − 4088.85 $^1P_1$	
$2s^22p^3$	$3p$	$^5P_1$:23211.9 $^5P_2$:23209.2 $^5P_3$:23205.8 $^3P_{0,1}$:21207.72 $^3P_2$:21207.16	$^3F_4$: −3876.09 $^3F_3$: −3883.02 $^3F_2$: −3888.70 $^3P_2$: −3456.43 $^3P_1$: −3459.83 $^1P_1$: −1620.2 $^3D_{1,2,3}$, $^1F_3$, $^1D_2$	$^3D_3$: −17443.83 $^3D_2$: −17449.49 $^3D_1$: −17452.90 $^3P_{0,1,2}$, $^3S_1$ $^1D_2$, $^1P_1$, $^1S_0$	
	$3d$	$^5D_{0,1,2,3,4}$:12417.3 $^3D_{1,2,3}$:12350.0	$^3G_{3,4,5}$, $^3F_{2,3,4}$, $^3D_{1,2,3}$, $^3P_{0,1,2}$ $^3S_1$ $^1G_4$, $^1F_3$, $^1D_2$, $^1P_1$ $^1S_0$	$^3F_{2,3,4}$, $^3D_{1,2,3}$, $^3P_{0,1,2}$ $^1F_3$, $^1D_2$, $^1P_1$	
$2s2p^4$	$2p$				$^3P_{0,1,2}$ $^1P_1$

the lines ascribed by Schniederjost to the oxygen arc spectrum are,—with the exception of λλ2895.37, 2883.93, 2858.81, 2708.18,—bands heads due to carbon compounds.

[4] J. C. McLennan, Proc. Roy. Soc. London **A120**, 327 (1928).
[5] W. Jevons, Phil. Mag. VI, **47**, 586 (1924); F. Paschen, Ann. d. Physik **23**, 261 (1907).
[6] C. Runge und F. Paschen, Ann. d. Physik **61**, 641 (1897).
[7] W. Schniederjost, Zeits. f. wiss. Phot. **2**, 283 (1904).
[8] W. Jevons, reference 4.

Since the intensity of the lines in the infra-red depends to so great an extent on the sensitizing of the plates, the intensities given are only comparable within the individual line groups.

Discussion

Table II and Fig. 1 give a summary of the terms to be expected on the Hund theory and those found. The diagram also shows the newly observed combinations. The term $2s^2\ 2p^3\ (^2D)\ 4p^3$: $D_{1,\ 2,\ 3}$ ($^3D_1 = 15949.12$, $^3D_2 = 15944.03$, $^3D_3 = 15936.64$) is not included in Table II.

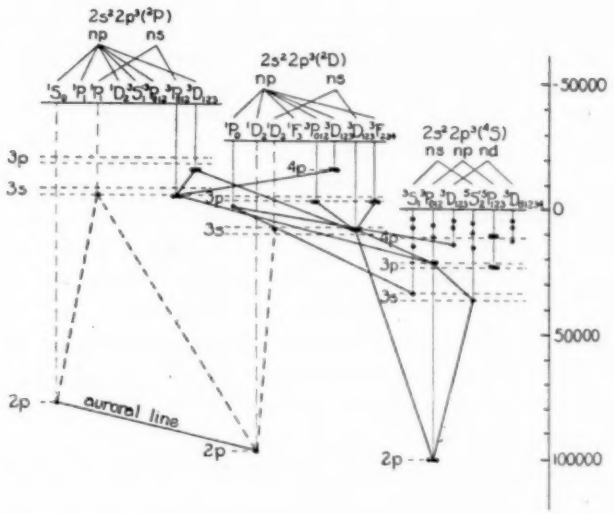

Fig. 1.

The oxygen arc spectrum is based on the deepest terms of the ion: $2s^22p^3:{}^4S$, $2s^22p^3:{}^2D$, $2s^22p^3:{}^2P$ and perhaps also $2s2p^4:{}^4P$ must be considered. The Runge-Paschen series as well as Hopfield's ultra-violet series are built on the deepest term of the ion: $2s^22p^3:{}^4S$. The deepest term ^3P is common to all three systems belonging to the configuration $2s^22p^3$.

On the basis of the very complete analysis of the O II spectrum by Fowler[9] and by Bowen[10] it is possible to predict the approximate position and separation of the arc terms. In the figure the approximate position of the terms $2s^22p^3(^1D)3s$, $2s^22p^3(^2D)3p$, $2s^22p^3(^2P)3s$ and $2s^22p^3(^2P)3p$ is indicated. They are located by displacing the Runge-Paschen terms $2s^22p^3(^4S)3s$, (^5S, ^3S) and $2s^22p^3\ (^4S)3p(^5P,\ ^3P)$ by the distance from the limit ^4S to the limits ^2D and ^2P respectively. It will be seen from the figure that the terms fall near the positions so determined.

The triplet separations give another indication of the correctness of the arrangement. The series limit of the ordinary Runge-Paschen series, the low

[9] A. Fowler, Proc. of the Roy. Soc. London **A110**, 476 (1926).
[10] J. S. Bowen, Phys. Rev. **29**, 242 (1927).

term ^4S of the ion is single which accounts for the relatively small separations of the triplet and quintet terms. The separations of the inverted terms of the ion $2s^22p^3:{}^2D$ and $2s^22p^3:{}^2P$ are 20 and 4.5 respectively. The new arc terms are also inverted and have the expected separations. In the term $2s^22p^3(^2D)3s:{}^3D$ the separation of the outer components is exactly 20 frequency units, for the other terms it is at least of the same order; in any case significantly greater than the separations of the Runge-Paschen terms.

The assignment of inner quantum numbers could in every case be made unambiguously from the observed combination. In one combination $2s^2 2p^3(^2D)3s:{}^3D - 2s^22p^3(^2P)3p:{}^3D$ two strong lines are missing. For the strongest line of this multiplet however there is an old Zeeman effect determination by Paschen and Back,[11] who observed a triplet of 4/3 normal separation. According to the table of anomalous Zeeman effect of Kiess and Meggers[12] this Zeeman effect is found only for the line $^3D_3 - {}^3D_3'$.

One two-fold term, -3459.83 and 3456.43, has been assumed to be an incompletely resolved ^3P term, in which the two components $^3P_0$ an $^3P_1$ fall together. These two terms do not appear to be two singlet terms since the combination with a ^3D term is very strong and since the five lines comprising this group under the most varied conditions of discharge seem in intensity and appearance to belong to one group.

A similar case is the Runge-Paschen term $2s^22p^3(^4S)3p^3:{}^3P$. The strong combination of this term with the term $2s^22p^3(^4S)3s:{}^3S$, the infra-red line λ8446A has previously always been observed as a narrow doublet and also in this investigation with the dispersion of 6.5 meter grating it was not possible further to resolve the stronger component of this doublet. (With the present mounting of the grating this line could not be photographed in the second order since the second order lay on the Rowland circle too close to the grating. The structure of the combinations of this term with the terms $2s^22p^3(^2D)3s:{}^3D$ and $2s^22p^3(^2P)3s:{}^3P$ showed that the two components $^3P_0$ and $^3P_1$ must fall together and that this term is normal and not inverted. It would be desirable in this connection to investigate the fine structure of this as well as of the next higher ^3P terms.

A narrow doublet at 6727A is given in the Table I as the intercombination between this ^3P term and the deepest ^5S term analogous to the intercombination observed by Hopfield between the deepest ^3P term and this ^5S term.

The remaining terms to be expected could not be located in the data available. Noticeably absent are the low $^3P-$ and $^1P-$ terms arising from the addition of an additional $2p$ electron to the $2s2p^4$ configuration of the ion. Such terms are known in the analogous spectra O III, N II, C I and give rise there to strong combinations. They are to be expected at about $-10{,}000$ cm^{-1} in O I. The strong characteristic group $2s^22p^4\,{}^3P - 2s2p^5\,{}^3P$ which should lie near 800A has never been observed in oxygen.

Among the unclassified lines in the table are the two inverted triplets at λ6260 and 5410A observed by Runge and Paschen. Although they show

[11] F. Paschen und E. Back, Ann. d. Physik **39**, 915 (1912).

[12] C. C. Kiess and W. F. Meggers, Journ. Res. Bureau of Standards **1**, 641 (1928).

exactly the separation of the triplet term $2s^22p^3(^2D)3s:{}^3D$ they are apparently not combinations of this term with negative singlet terms. For in discharges in narrow capillaries both triplets as also observed by Runge and Paschen appear with the central line far exceeding the other two in intensity. On the contrary in discharges in a mixture of a small percentage of oxygen in helium the central component is weaker than the other two. It was impossible to resolve the central line and an explanation of this intensity variation does not appear. Among the lines in the Table I are also two wider triplets at 5730 and 4220A which both have the separations 58 and 32 cm^{-1}. No other combinations of the terms common to these triplets have been observed.

The two low terms $2s^22p^4:{}^1D$ and $2s^22p^4:{}^1S$ are of especial interest. According to McLennan[13] the green auroral line 5577.350 is the forbidden transition between these terms. Even the position of these terms is unknown. The classification is supported on one side by the analogous explanation of the nebular lines by Bowen [14] and on the other by the observation of the Zeeman effect of this line made by McLennan[13] and confirmed by Sommer.[15]

Various attempts have been made to fix the location of these terms. Hopfield[16] has shown that the ultra-violet lines λλ999.47 and 1217.62 have exactly for frequency difference the freqeuncy of the auroral line, and are thus combinations of these two terms with a third term. Cario[17] and also Kaplan[18] have given approximate values for the position of these two terms ^1D and ^1S on the basis that the distance of the deeper of the two terms from the lowest term ^3P cannot be greater than the difference between this lowest term and the frequency of the shorter of the Hopfield lines, in order that the two lines may fit in the term scheme of the oxygen arc spectrum. They overlook thus the fact, that this higher term may lie higher than the deepest ionizing limit and so be negative.

The green auroral line appears strongly in mixtures of helium, neon or argon with oxygen but fails to be excited according to Cario[17] in mixtures of krypton and oxygen. Although much has been learned in recent years of the excitation process in mixtures of the noble gases and other gases, it is still not possible on the basis of the above mentioned observations to make any precise assertions over the excitation potential of the green auroral line, since the energy required for dissociation preceding this excitation is not known.

A relatively plausible approximation of the location of the metastable terms may be made by comparison[15] with the similarly constructed O III spectrum. There also are found in it the same term configurations consisting of a ^3P term as lowest term and two slightly higher metastable singlet terms ^1D and ^1S. The "forbidden" combinations between these terms give according

[13] J. C. McLennan, Proc. Roy. Soc. London **A120,** 327 (1928).
[14] I. S. Bowen, Astrophys. J. **67,** 1 (1928).
[15] L. A. Sommer, Zeits. f. Physik **51,** 451 (1928).
[16] J. J. Hopfield, Phys. Rev. **29,** 923 (1927).
[17] G. Cario, Journal Franklin Institution **205,** 515 (1928).
[18] J. Kaplan, Proc. Nat. Acad. Amer. **14,** 882 (1928).

to Bowen[14] known nebular lines and the difference $^3P-{}^1D$ is less then $^1D-{}^1S$. If the location of the deepest terms in O I is analogous, the difference $^3P-{}^1D$ would be about 15,500 cm^{-1}.

We have as yet not investigated the extreme ultra-violet. Thus it is not possible to look for other combinations of these terms with higher terms. However by the determination of the terms $2s^22p^3(^2D)3s:{}^3D$ and $2s^22p^3(^2P)3s:{}^3P$ the approximate position of the singlet terms $2s^22p^3(^2D)3s:{}^1D$ and $2s^22p^3(^2P)3s:{}^1P$ is fixed. The two above mentioned lines found by Hopfield $\lambda\lambda$999.47 and 1217.62 as well as a further strong unclassified oxygen arc lines at 1152.0 have therefore been included in the level figure as combinations between the metastable terms and these singlet terms. One obtains thus an estimate of the position of the metastable terms which agrees with that found by comparison with the O III spectrum. The definitive explanation of these terms is held in abeyance pending the conclusion of a projected investigation of the ultra-violet oxygen spectrum.

In conclusion the writer wishes to express his appreciation to the International Education Board for the grant of a Fellowship; to Professor H. M. Randall for the facilities extended him, and to Professor R. A. Sawyer and Dr. S. B. Ingram for helpful suggestions and discussions.

THE RELATIVE INTENSITIES OF NEBULAR LINES

By James H. Bartlett, Jr.

Physikalisches Institut, Eidgenössische Technische Hochschule, Zürich

(Received August 31, 1929)

Abstract

It is proved rigorously for multipole radiation that the transition $j=0\rightarrow j=0$ cannot occur. The relative intensities of the lines of the multiplet $^2P\rightarrow{}^2D$ are calculated. They are in the ratio $3/2\rightarrow5/2:1/2\rightarrow3/2:3/2\rightarrow3/2:1/2\rightarrow5/2=10:5:2:1$, approximately. This is not in agreement with experiment in that the weaker lines are not observed. The relative intensities of the intercombination lines comprising the multiplet $^1D\rightarrow{}^3P$ are calculated, using in part the Darwin-Pauli theory of the spinning election as applied by Houston to the study of intercombination lines. The line $^1D_2\rightarrow{}^3P_2$ always is strongest according to the calculations, and the experiments confirm this. The line $^1D_2\rightarrow{}^3P_1$ is about half as strong, which also checks experiment. The intensity of $^1D_2\rightarrow{}^3P_0$ varies, however, from zero to a value of the same order of magnitude as that of $^1D_2\rightarrow{}^3P_1$. This is in disagreement with experiment in that the line is not observed. This is the same sort of disagreement as for the multiplet $^2P\rightarrow{}^2D$. It is concluded that Bowen's hypothesis, attributing the emission of the "forbidden" nebular lines to quadrupole radiation, is substantiated to some extent, but not fully. The discrepancies between theory and experiment may arise from the simplifying assumptions introduced.

CERTAIN lines in nebular spectra have been interpreted[1] as due to transitions in O III, N II, O II and S II,[2] occurring in violation of Laporte's rule. According to theory,[3] these lines can only be emitted either when an electric field (or an inhomogeneous magnetic field) is present, or when the atom is left undisturbed for a time long enough that quadrupole radiation[4] can become effective. The first possibility has been considered[1] and found to be improbable, due to the non-observation of a broadening of the Balmer lines such as would be expected. Accordingly, the other alternative (corresponding to the hypothesis of Bowen) is treated in the present paper. The rigorous handling of this problem would require calculations of a complication hardly justifiable, but it is hoped that the work here presented is sufficient to warrant a qualitative conclusion. In particular, we cannot give the relative transition probabilities from the normal state to excited states corresponding to different electronic configurations (such as $(2s)^2 2p3s$ and $2s2p^3$ in O III). It should be remarked in passing that the emission

[1] For a full discussion, see F. Becker u. W. Gotrian, Ergebnisse der exakten Naturwissen schaften, Bd. **7**, 8 ff. (1928).

[2] I. S. Bowen, Nature **123**, 450 (1929).

[3] E. Wigner, Zeits. f. Physik **43**, 624 (1927) and **45**, 601 (1927). Also J. v. Neumann and E. wigner, Zeits f. Physik **49**, 91 (1928).

[4] For the development of the theory, see I. I. Placinteanu, Zeits. f. Physik **39**, 276 (1926) and J. Frenkel, Elektrodynamik (1926) Bd. I, p. 93. Also see A. Rubinowicz. Zeits. f. Physik **53**, 267 (1929). This will be referred to as l.c.

of forbidden lines, in the optical region, under conditions that subsist in the laboratory, must have another cause than quadrupole radiation, for to talk of an undisturbed atom in this case would be absurd. On the other hand, it may be possible to ascribe the emission of forbidden x-ray lines to quadrupole radiation, since the action of external disturbances for the inner electrons is much smaller and since the quadrupole radiation is much greater because the wave-length is comparable with the atomic radius.[5]

It was possible for Rubinowicz[4] to show that the radiation in any given direction from a multipole has, at large distances, the properties of a plane wave. The intensity of radiation in the z direction is determined by the time mean of the z component of the Poynting vector S, so that if A is the vector potential, and A^* its complex conjugate, we have:

$$(\bar{z}S)=\frac{ck^2}{8\pi}[\bar{z}A][\bar{z}A^*]=\frac{ck^2}{8\pi}(A_xA_x^*+A_yA_y^*)$$

$$=\frac{ck^2}{8\pi}\cdot\frac{1}{2}[(A_x+iA_y)(A_x+iA_y)^*+(A_x-iA_y)(A_x-iA_y)^*]$$

where c = velocity of light, ν = frequency of emitted light, $k=2\pi\nu/c$, and $\bar{z}$ denotes a unit vector in the z direction. From formula (2) of Rubinowicz,[4]

$$A_x=\frac{1}{c}\int\frac{e^{-ikR}}{R}i_x d\tau$$

where the time factor $e^{2\pi i\nu t}$ is omitted, i_x signifies the component of current in the x direction, and R is the distance from the source of radiation to the point under consideration. Let r be the distance from the center of the atom to this same point.

Then

$$A_x\cong\frac{1}{c}\,\frac{e^{-ikr}}{r}\int i_x e^{ikz}d\tau$$

Expanding in series, and letting $i=ep/m$, where p is the momentum,

$$A_x=\frac{e}{mc}\,\frac{e^{-ikr}}{r}\left[\int p_x d\tau+\int ik(zp_x)d\tau+\cdots\right]$$

The first term gives the part due to dipole radiation (Rubinowicz[4] p. 272) the second that due to quadrupole radiation (l.c., formula (14), $p=1$), and so on. Thus, we shall deal with matrix elements of the types p, zp, z^2p, etc. For quadrupole radiation, therefore,

$$A_x+iA_y\sim z(p_x+ip_y)\ ;\quad A_x-iA_y\sim z(p_x-ip_y).$$

The problem then essentially reduces to calculating the matrix amplitudes of $z(p_x+ip_y)$ with aid of the relation

$$[z(p_x+ip_y)]^{n,l,j,m}_{n,l',j',m-1}=\sum_{n'l''j''}z^{n,l,j,m}_{n',l'',j'',m}(p_x+ip_y)^{n',l'',j'',m}_{n,l',j',m-1}$$

[5] I owe this suggestion to Professor W. Pauli, Jr.

where the summation is to be taken over all such intermediate states as are accessible both from the end state $(n, l', j'. m-1)$ as well as from the initial state(n, l, j, m).

I. Quadrupole Radiation Between States of the Same Multiplicity

The following formulae[6] are necessary for our calculation:

a. Zeeman Lines.

$$A^{m,j}_{m\pm1,j}=\frac{A^j_j}{j(j+1)}\ \frac{1}{2}(j\mp m)(j\pm m+1)\ ;\ A^{m,j}_{m,j}=\frac{A^j_j}{j(j+1)}m^2$$

$$A^{m,j}_{m\pm1,j+1}=\frac{A^j_{j+1}}{(j+1)(2j+3)}\ \frac{1}{2}(j\pm m+2)(j\pm m+1)\ ;$$

$$A^{m,j}_{m,j+1}=\frac{A^j_{j+1}}{(j+1)(2j+3)}[(j+1)^2-m^2]$$

$$A^{m,j}_{m\pm1,j-1}=\frac{A^j_{j-1}}{j(2j-1)}\ \frac{1}{2}(j\mp m)(j\mp m-1)\ ;$$

$$A^{m,j}_{m,j-1}=\frac{A^j_{j-1}}{j(2j-1)}(j^2-m^2)$$

b. Multiplet Lines.

$$\Delta l=-1\ \begin{cases} J_{-1}=G_j\ \ A^{j,l}_{j-1,l-1}=\dfrac{C}{4jl}P(j,l)P(j-1,l) \\ J_0=G_j\ \ A^{j,l}_{j,l-1}\ =C\dfrac{2j+1}{4jl(j+1)}P(j,l)Q(j,l) \\ J_{+1}=G_{j-1}A^{j-1,l}_{j,l-1}\ =\dfrac{C}{4jl}Q(j,l)Q(j-1,l) \end{cases}$$

$$\Delta l=0\ \begin{cases} J_0=G_j\ \ A^{j,l}_{j,l}\ \ =\dfrac{C}{4jl}\ \dfrac{2l+1}{l+1}\ \dfrac{2j+1}{j+1}R^2(j,l) \\ J_{\pm1}=G_j\ \ A^{j,l}_{j-1,l}\ =G_{j-1}A^{j-1,l}_{j,l}=\dfrac{C}{4jl}\ \dfrac{2l+1}{l+1}P(j,l)Q(j-1,l) \end{cases}$$

$$\Delta l=+1\ \begin{cases} J_{-1}=G_j\ \ A^{j,l}_{j-1,l+1}=\dfrac{C}{4j(l+1)}Q(j,l+1)Q(j-1,l+1) \\ J_0=G_j\ \ A^{j,l}_{j,l+1}\ =\ \dfrac{C}{4j(l+1)}\ \dfrac{2j+1}{j+1}P(j,l+1)Q(j,l+1) \\ J_{+1}=G_{j-1}A^{j-1,l}_{j,l+1}\ =\dfrac{C}{4j(l+1)}P(j,l+1)P(j-1,l+1). \end{cases}$$

[6] See W. Pauli, Handbuch der Physik, Bd. XXIII, p. 67 and p. 243 in particular, and the accompanying text, for a thoroughgoing discussion.

Here are made the following abbreviations:

$$P(j,l)=(j+l)(j+l+1)-s(s+1)$$
$$-Q(j,l)=(j-l)(j-l+1)-s(s+1)$$
$$R(j,l)=j(j+1)+l(l+1)-s(s+1)$$

where $s=0$ for singlets, $\frac{1}{2}$ for doublets, etc.
One verifies readily that

$$P(j,l)=R(j,l)+2jl$$
$$-Q(j,l)=R(j,l)-2(j+1)l.$$

The A's above are squares of matrix amplitudes.

Now let $v=x+iy$, $p_v=p_x+ip_y$, $w=x-iy$, $p_w=p_x-ip_y$.

In the calculations, products of the form $AB=z_b^a v_c^b z_e^d v_f^e$ occur, where the letters a to f denote values which the inner quantum number takes on. Such products are listed in Table I. $(AB=BA)$

TABLE I. *Products AB.*

B \ A	$z^j_{j-1}v^{j-1}_j$	$z^j_j v^j_j$	$z^j_{j+1}v^{j+1}_j$
$z^j_{j-1}v^{j-1}_j$	$\dfrac{(j^2-m^2)(j-m+1)(j-m)}{j^2(2j-1)(2j+1)}$		
$z_j{}^j v_j$	$\dfrac{(j^2-m^2)(j-m+1)m}{j^2(j+1)[(2j-1)(2j+1)]^{1/2}}$	$\dfrac{m^2(j+m)(j-m+1)}{[j(j+1)]^2}$	
$z^j_{j+1}v^{j+1}_j$	$\dfrac{(j^2-m^2)(j-m+1)(j+m+1)}{j(j+1)(2j+1)[(2j-1)(2j+3)]^{1/2}}$	$\dfrac{m(j+m)(j-m+1)(j+m+1)}{j(j+1)^2[(2j+1)(2j+3)]^{1/2}}$	$\dfrac{(j+m)(j-m+1)(j+m+1)^2}{(2j+3)(2j+1)(j+1)^2}$

B \ A	$z^j_j v^j_{j+1}$		B \ A	$z^j_{j+1}v^{j+1}_{j+2}$
$z^j_j v^j_{j+1}$	$\dfrac{m^2(j-m+2)(j-m+1)}{j(j+1)^2(2j+3)}$		$z^j_{j+1}v^{j+1}_{j+2}$	$\dfrac{(j-m+1)(j+m+1)(j-m+1)(j-m+2)}{(j+1)(j+3)(2j+3)(2j+5)}$
$z^j_{j+1}v^{j+1}_j$	$\dfrac{m(j-m+1)(j-m+2)(j+m+1)}{(j+1)^2(2j+3)[j(j+2)]^{1/2}}$	$\dfrac{(j-m+1)(j+m+1)^2(j-m+2)}{(2j+3)(j+1)^2(j+2)}$		

The procedure is to determine $[(zp_v)^{n,l,j,m}_{n,l',j';m-1}]^2$ and then to sum over m to eliminate the effect of spacial degeneracy. Natural excitation is assumed to be the case.

Let

$$\tau(j)=\frac{3j^2+3j-1}{5}.$$

The products AB given above are dependent on m. We sum them over all possible values of m. The results are given in Table II

In the case of the multiplet ${}^2P\rightarrow{}^2D$, the intermediate state can be either a $P-$state or a $D-$state. We shall calculate the relative intensities of the

TABLE II. $\Sigma_m[AB]^2(m)$

B \ A	$z^{j}_{j-1}v_j^{j-1}$	$z_j^j v_j^j$	$z^{j}_{j+1}v_j^{j+1}$
$z_{j-1}^j v_j^{j-1}$	$\frac{1}{3(2j+1)}\left[3j^2+2j+1-\frac{j-1}{j}\tau(j-1)\right]$		
$z_j^j v_j^j$	$-\frac{1}{3}\frac{j(j-1)}{j+1}\left[\frac{2-1j}{2j+1}\right]^{1/2}\left[1-\frac{\tau(j-1)}{j^2}\right]$	$\frac{2j^2+\frac{1}{2}(j-1)(2j-1)[j(j+1)-\tau(j-1)]}{j(j+1)^2}$	
$z_{j+1}^j v_j^{j+1}$	$\frac{1}{3}\left[\frac{2j-1}{2j+3}\right]^{1/2}\left[j+1+\frac{-1}{(j+1)(2j+1)}[\tau(j-1)-j^2]\right]$	$\frac{\frac{1}{2}(j-1)(2^j-1)[(j+1)^2-\tau(j-1)]+2j(2j+1)}{(j+1)^2[(2j+1)(2j+3)]^{1/2}}$	$\frac{\frac{1}{2}j(j-1)(2j-1)[(j+1)^2-\tau(j-1)]+2j(2j+1)^2+j(2j-1)(j+1)^2}{(j+1)^2(2j+1)(2j+3)}$

B \ A	$z_j^j v_j^{j+1}$	$z^{j}_{j+1}v_j^{j+1}$
$z_j^j v_j^{j+1}$	$\frac{1}{3}\frac{2j+1}{(j+1)(2j+3)}[(j+1)(j+2)+\tau(j)]$	
$z^{j}_{j+1}v_{j+1}^{j+1}$	$\frac{1}{3}\frac{j(2j+1)[\tau(j)-(j+1)^2]}{(j+1)(2j+3)[j(j+2)]^{1/2}}$	$\frac{1}{3}\frac{2j+1}{(2j+3)(j+1)(j+2)}[(j+1)(j^2+j6+6)+j\tau(j)]$

B \ A	$z^{j}_{j+1}v_{j+2}^{j+1}$
$z^{j}_{j+1}v_{j+2}^{j+1}$	$\frac{-\frac{1}{2}j(2j+1)[\tau(j)+3j+5]+(j+1)(j+2)(j+3)}{(j+2)\,(\,2j+3)\,(\,2j+5)}$

lines of this multiplet assuming (1) that there is one intermediate $P-$state effective and (2) that there is one intermediate $D-$state effective.

A sample calculation for the line $^2P_{1/2}\rightarrow{}^2D_{3/2}$ follows.

Case (I).

$$(zp_v)^{n,1,1/2,m}_{n,2,3/2,m-1}=z^{n,1,1/2,m}_{n',1,1/2,m}\,p^{n',1,1/2,m}_{vn,2,3/2,m-1}+z^{n,1,1/2,m}_{n',1,3/2,m}\,p^{n',1,3/2,m}_{vn,2,1/2,m-1}.$$

Using the relation

$$p^{n',1}_{vn,2}=2\pi i m\nu^{n',1}_{n,2}\,v^{n',1}_{n,2}$$

we calculate that

$$\sum[zp_v]^2(m)\sim(\nu^{n',1}_{n,2})^2\left\{\frac{4}{9}A^{n,1,1/2}_{n',1,1/2}A^{n',1,1/2}_{n,2,3/2}+\frac{28}{45}A^{n,1,1/2}_{n',1,3/2}A^{n',1,3/2}_{n,2,3/2}\right.$$

$$\left.-\frac{4}{9(5)^{1/2}}\left(A^{n,1,1/2}_{n',1,1/2}A^{n',1,1/2}_{n,1,3/2}A^{n',1,1/2}_{n,2,3/2}A^{n',1,3/2}_{n,2,3/2}\right)^{1/2}\right\}$$

$$=(\nu^{n',1}_{n,2})^2A^{n,1}_{n',1}A^{n',1}_{n,2}\left(\frac{40}{9}+\frac{14}{45}-\frac{4}{9}\right)=4.3(\nu^{n',1}_{n,2})^2A^{n,1}_{n',1}A^{n',1}_{n,2}.$$

The relative intensities are then as follows:

$$3/2\rightarrow5/2:1/2\rightarrow3/2:3/2\rightarrow3/2:1/2\rightarrow5/2=10.8:4.3:2.8:1.8$$

Case (2).

The relative intensities when a $D-$state is intermediate are

$$3/2\rightarrow5/2:1/2\rightarrow3/2:3/2\rightarrow3/2:1/2\rightarrow5/2=23.8:14:4:1$$

Only the line $^2P_{1\frac{1}{2}}\rightarrow{}^2D_{2\frac{1}{2}}$ is observed experimentally. It is to be noted that the transition $j=\frac{1}{2}\rightarrow j=2\frac{1}{2}$ is especially weak, as one would expect. This calculation is in error insofar as it leaves out of account the effect of the possible intermediate state $2s2p^4\,{}^4P$, which lies so low that it may have some influence. Transitions to and from this state would, however, be intercombinations, and so it is believed that its effect is quite negligible.

Since m must change[7] by ±1, it is a trivial conclusion that the transition $j=0\rightarrow j=0$ cannot occur for multipole radiation. A corresponding rule,[8] which is not exact in that it neglects the interaction of angular momenta of spin and orbit, states that the transition $l=0\rightarrow l=0$ cannot occur. The rule for the inner quantum number, is however, perfectly rigorous (for multipole radiation). When, however, electric fields or similar influences are present, then both of the above rules will be violated.

II. Dipole Radiation for Intercombinations Between States of Different Multiplicities

1. *The Secular Equations and Perturbed Wave Functions.* To calculate quadrupole radiation for intercombination lines, we must first know the

[7] This follows from the fact that the matrix elements are of the type z^np, as already stated.

[8] A. Rubinowicz, Phys. Zeits. **29**, 823 (1928).

dipole radiation to or from the intermediate state. It is simplest to treat as intermediate states those arising from the $2p3s$ configuration. The $2p\ 3d$ configuration can probably be neglected, since the combinations with the ground state are rather weak. As to $2s\ 2p$,[3] a straightforward method of attact such as employed for $2p\ 3s$ is much too complicated to be worthwhile. For this reason, the present paper deals only with $2p\ 3s$. A short discussion of $2s\ 2p^3$ is given later.

To calculate the dipole radiation, we make use of the method developed by Houston[9] for determining the wave functions which result from the disturbance of symmetry coming from the mutual interaction between the angular momenta of spin and orbit. The function of the co-ordinates of one electron may be written as $R_{ln}^{(r)}\ P_l^{m_l}$, where l is the azimuthal quantum number, and m_l its projection on a prefered axis. Also,

$$P_l^{m_l} = (l-m_l)!\ \sin^{m_l}\theta \left(\frac{d}{d\cos\theta}\right)^{l+m_l} \frac{(-\sin^2\theta)^l}{2^l l!}\ e^{\ im_l\phi}$$

The two possible values of the spin variable are denoted by S_α and S_β, respectively. The perturbing energy arises (1) from the electrostatic interaction of the two electrons and (2) from two magnetic interactions, namely between the spin of each electron and its orbit. As unperturbed wave functions of $(2p)^2$, we take the following[10]:

$$\psi_\alpha^{\,2} = (\tfrac{1}{2})^{1/2}\{P_1^0(1)P_1^1(2) - P_1^0(2)P_1^1(1)\}S_\alpha(1)S_\alpha(2)$$
$$\psi_\epsilon^{\,2} = (\tfrac{1}{2})^{1/2}P_1^1(1)P_1^1(2)\{S_\alpha(1)S_\beta(2) - S_\beta(1)S_\alpha(2)\}$$

$$\psi_\alpha^{\,1} = (\tfrac{1}{2})^{1/2}\{P_1^{-1}(1)P_1^1(2) - P_1^{-1}(2)P_1^1(1)\}S_\alpha(1)S_\alpha(2)$$
$$\psi_\gamma^{\,1} = \tfrac{1}{2}\{P_1^0(1)P_1^1(2) - P_1^0(2)P_1^1(1)\}\{S_\alpha(1)S_\beta(2) + S_\beta(1)S_\alpha(2)\}$$
$$\psi_\delta^{\,1} = \tfrac{1}{2}\{P_1^0(1)P_1^1(2) + P_1^0(2)P_1^1(1)\}\{S_\alpha(1)S_\beta(2) - S_\beta(1)S_\alpha(2)\}$$

$$\psi_\alpha^{\,0} = (\tfrac{1}{2})^{1/2}\{P_1^0(1)P_1^1(2) - P_1^0(2)P_1^1(1)\}S_\beta(1)S_\beta(2)$$
$$\psi_\beta^{\,0} = (\tfrac{1}{2})^{1/2}\{P_1^0(1)P_1^{-1}(2) - P_1^0(2)P_1^{-1}(1)\}S_\alpha(1)S_\alpha(2)$$
$$\psi_\gamma^{\,0} = \tfrac{1}{2}\{P_1^{-1}(1)P_1^1(2) - P_1^{-1}(2)P_1^1(1)\}\{S_\alpha(1)S_\beta(2) + S_\beta(1)S_\alpha(2)\}$$
$$\psi_\delta^{\,0} = \tfrac{1}{2}\{P_1^{-1}(1)P_1^1(2) + P_1^{-1}(2)P_1^1(1)\}\{S_\alpha(1)S_\beta(2) - S_\beta(1)S_\alpha(2)\}$$
$$\psi_\epsilon^{\,0} = (\tfrac{1}{2})^{1/2}P_1^0(1)P_1^0(2)\{S_\alpha(1)S_\beta(2) - S_\beta(1)S_\alpha(2)\}$$

$$\psi_\alpha^{-1} = (\tfrac{1}{2})^{1/2}\{P_1^{-1}(1)P_1^1(2) - P_1^{-1}(2)P_1^1(1)\}S_\beta(1)S_\beta(2)$$
$$\psi_\gamma^{-1} = \tfrac{1}{2}\{P_1^0(1)P_1^{-1}(2) - P_1^0(2)P_1^{-1}(1)\}\{S_\alpha(2)S_\beta(2) + S_\beta(1)S_\alpha(2)\}$$
$$\psi_\delta^{-1} = \tfrac{1}{2}\{P_1^0(1)P_1^{-1}(2) + P_1^0(2)P_1^{-1}(1)\}\{S_\alpha(1)S_\beta(2) - S_\beta(1)S_\alpha(2)\}$$

$$\psi_\alpha^{-2} = (\tfrac{1}{2})^{1/2}\{P_1^0(1)P_1^{-1}(2) - P_1^0(2)P_1^{-1}(1)\}S_\beta(1)S_\beta(2)$$
$$\psi_\epsilon^{-2} = (\tfrac{1}{2})^{1/2}P_1^{-1}(1)P_1^{-1}(2)\{S_\alpha(1)S_\beta(2) - S_\beta(1)S_\alpha(2)\}.$$

[9] W. V. Houston, Phys. Rev. **33**, 297 (1929).
[10] See J. A. Gaunt, Phil. Trans. **A228**, 184 (1929) for similar functions.

The common radial function is not written. The superscript of ψ specifies $m=\sum m_l+m_s$, the quantum number corresponding to the projection of the angular momentum in a fixed direction, which is a constant of the motion when the atom is not subject to an external field. The subscript of ψ serves to distinguish between functions with the same m. Since, for an undisturbed atom, terms with different m cannot combine, the original fifteen-rowed secular equation may be broken up into (1) two equivalent two-rowed equations, (2), two equivalent three-rowed equations, and (3) one five-rowed equation. From (1), one solves for the energy levels which are consistent with $m=2$ and these are $^1D_2$ and $^3P_2$. One also has a possibility of $m=1$ for these, and so from (2) we obtain them and $^3P_1$ in addition. From (3), we obtain all the energy levels, namely $^1D_2$, $^3P_{0,1,2}$, and $^1S_0$.

The procedure adopted here is to start out with wave functions which are correct zeroth approximations if only the electrostatic interaction of the electrons is considered. Of these functions written above, ψ_δ^0 and ψ_ϵ^0 are not such. Applying a perturbation calculation,[11] the perturbation being the electrostatic interaction, we find for the proper wave functions,

$$^1D_2\colon\ \psi_{\mathrm{IV}}^0=(\tfrac{1}{3})^{1/2}\psi_\delta^0+(\tfrac{2}{3})^{1/2}\psi_\epsilon^0$$
$$^1S_0\colon\ \psi_{\mathrm{V}}^0=-(\tfrac{2}{3})^{1/2}\psi_\delta^0+(\tfrac{1}{3})^{1/2}\psi_\epsilon^0$$

The problem is then to find linear combinations which are correct zeroth approximations when the magnetic interaction resulting in the splitting-up of the multiplet is taken into account.

If we define

$$\gamma_{12}=\frac{h^2}{16\pi^2}\,\frac{ze^2}{m_0^2c^2}\int R_{12}^2\frac{1}{r^3}d\tau$$

and

$$Y_1=\frac{\Delta E_1}{\gamma_{12}}\ ;\quad Y_2=\frac{\Delta E_2}{\gamma_{12}}\ ;\quad \epsilon=\frac{\Delta E}{\gamma_{12}}$$

where ΔE_1 and ΔE_2 are the excitation energies of $^1D_2$ and $^1S_0$, respectively, then it is possible to write the secular equation for $m=0$ as follows:

$$\begin{vmatrix} -1-\epsilon & 0 & 1 & -(1/3)^{1/2} & -(8/3)^{1/2} \\ 0 & -1-\epsilon & -1 & (1/3)^{1/2} & (8/3)^{1/2} \\ 1 & -1 & -\epsilon & -(4/3)^{1/2} & (8/3)^{1/2} \\ -(1/3)^{1/2} & (1/3)^{1/2} & -(4/3)^{1/2} & Y_1-\epsilon & 0 \\ -(8/3)^{1/2} & (8/3)^{1/2} & (8/3)^{1/2} & 0 & Y_2-\epsilon \end{vmatrix}=0$$

The energies are measured from a zero between the two outer triplet terms, which would be the energy of the unresolved triplet.

[11] This is in every respect the same as that of Gaunt (ref. 10) except that we use normalized functions.

The calculation may be simplified[12] by considering the triplet by itself and finding the wave functions for the various values of j (in zeroth approximation). Thus, for $m=0$, we solve the secular equation:

$$\begin{vmatrix} -1-\epsilon & 0 & 1 \\ 0 & -1-\epsilon & -1 \\ 1 & -1 & -\epsilon \end{vmatrix} = 0$$

obtaining as roots $\epsilon_1=-2$, $\epsilon_2=-1$, $\epsilon_3=1$ and as wave functions

$$\epsilon_3: {}^3P_2: \psi_\mu{}^0 = (\tfrac{1}{6})^{1/2}(\psi_\alpha{}^0 - \psi_\beta{}^0 + 2\psi_\gamma{}^0)$$
$$\epsilon_2: {}^3P_1: \psi_\lambda{}^0 = (\tfrac{1}{2})^{1/2}(\psi_\alpha{}^0 + \psi_\beta{}^0)$$
$$\epsilon_1: {}^3P_0: \psi_\kappa{}^0 = (\tfrac{1}{3})^{1/2}(\psi_\alpha{}^0 - \psi_\beta{}^0 - \psi_\gamma{}^0).$$

Then, for $j=2$

$$\begin{array}{c|cc} & \psi_\mu{}^0 & \psi_{\mathrm{IV}}{}^0 \\ \psi_\mu{}^0 & 1-\epsilon & -2^{1/2} \\ \psi_{\mathrm{IV}}{}^0 & -2^{1/2} & Y_1-\epsilon \end{array} = 0$$

and for $j=0$

$$\begin{array}{c|cc} & \psi_\kappa{}^0 & \psi_{\mathrm{V}}{}^0 \\ \psi_\kappa{}^0 & -2-\epsilon & -2(2)^{1/2} \\ \psi_{\mathrm{V}}{}^0 & -2(2)^{1/2} & Y_2-\epsilon \end{array} = 0$$

The roots become:

$${}^1S_0: \epsilon_5 = (\tfrac{1}{2})\left[Y_2 - 2 + \left\{(Y_2+2)^2+32\right\}^{1/2}\right]$$
$${}^1D_2: \epsilon_4 = (\tfrac{1}{2})\left[Y_1 + 1 + \left\{(Y_1-1)^2-8\right\}^{1/2}\right]$$
$${}^3P_2: \epsilon_3 = (\tfrac{1}{2})\left[Y_1 + 1 - \left\{(Y_1-1)^2-8\right\}^{1/2}\right]$$
$${}^3P_1: \epsilon_2 = -1$$
$${}^3P_0: \epsilon_1 = (\tfrac{1}{2})\left[Y_2 - 2 - \left\{(Y_2+2)^2+32\right\}^{1/2}\right]$$

The wave functions are:

$m=2$

$${}^1D_2: (1/c_4\Delta_2)^{1/2}(-2^{1/2}\psi_\alpha{}^2 + c_4\psi_\epsilon{}^2)$$
$${}^3P_2: (1/c_3\Delta_2)^{1/2}(2^{1/2}\psi_\alpha{}^2 + c_3\psi_\epsilon{}^2)$$

$m=1$

$${}^1D_2: (1/c_4\Delta_2)^{1/2}(-\psi_\alpha{}^1 - \psi_\gamma{}^1 + c_4\psi_\delta{}^1)$$
$${}^3P_2: (1/c_3\Delta_2)^{1/2}(\psi_\alpha{}^1 + \psi_\gamma{}^1 + c_3\psi_\delta{}^1)$$
$${}^3P_1: (1/2)^{1/2}(-\psi_\alpha{}^1 + \psi_\gamma{}^1)$$

[12] This became apparent during a discussion of the matter with Dr. L. L. Rosenfeld whom I wish to thank for his helpfulness.

$m=0$

$$^1S_0:(1/c_5\Delta_0)^{1/2}(2\cdot 2^{1/2}\psi_\kappa{}^0+c_5\psi_{\mathrm{V}}{}^0)$$
$$^1D_2:(1/c_4\Delta_2)^{1/2}(-2^{1/2}\psi_\mu{}^0+c_4\psi_{\mathrm{IV}}{}^0)$$
$$^3P_2:(1/c_3\Delta_2)^{1/2}(2^{1/2}\psi_\mu{}^0+c_3\psi_{\mathrm{IV}}{}^0)$$
$$^3P_1:(1/2)^{1/2}(\psi_\alpha{}^0+\psi_\beta{}^0)$$
$$^3P_0:(1/c_1\Delta_0)^{1/2}(2\cdot 2^{1/2}\psi_\kappa{}^0-c_1\psi_{\mathrm{V}}{}^0)$$

$m=-1$

$$^1D_2:(1/c_4\Delta_2)^{1/2}(-\psi_\alpha{}^{-1}+\psi_\gamma{}^{-1}+c_4\psi_\delta{}^{-1})$$
$$^3P_2:(1/c_3\Delta_2)^{1/2}(\psi_\alpha{}^{-1}-\psi_\gamma{}^{-1}+c_3\psi_\delta{}^{-1})$$
$$^3P_1:(1/2)^{1/2}(\psi_\alpha{}^{-1}+\psi_\gamma{}^{-1})$$

$m=-2$

$$^1D_2:(1/c_4\Delta_2)^{1/2}(2^{1/2}\psi_\alpha{}^{-2}+c_4\psi_\epsilon{}^{-2})$$
$$^3P_2:(1/c_3\Delta_2)^{1/2}(-2^{1/2}\psi_\alpha{}^{-2}+c_3\psi_\epsilon{}^{-2}).$$

In these formulae, Δ_j means the separation, in terms of ϵ, of the two levels with the same j. Thus: $\Delta_0=|\epsilon_5-\epsilon_1|$. For brevity we have written

$$c_1=|2+\epsilon_1|,\qquad c_5=|2+\epsilon_5|,\qquad c_3=|1-\epsilon_3|,\qquad \text{and}\qquad c_4=|1-\epsilon_4|$$

One finds that

$$c_1c_5=8 \text{ and } c_3c_4=2.$$ When Y_1 and Y_2 are large, $c_5\cong\Delta_0$, $c_4\cong\Delta_2$.

For the case where interaction between spin and orbit is negligible, the triplet has the 2:1 ratio of separations. When the interaction between the electrons is zero, (that is, $Y_1=Y_2=0$), $\epsilon_1=-4$, $\epsilon_2=\epsilon_3=-1$, $\epsilon_4=\epsilon_5=2$, or the $^1S_0$ and $^1D_2$ levels merge [13] together, as do the $^3P_2$ and $^3P_1$ levels. The quintet degenerates into a triplet with separation ratio 1:1. In the case treated by Houston, neighboring levels such as $^1P_1$ and $^3P_2$ and $^3P_1$ and $^3P_0$ merged together likewise.

Following Houston, let

$$\gamma_{ln}=\frac{h^2}{16\pi^2}\,\frac{Ze^2}{m_0{}^2c^2}\int R_{ln}{}^2\frac{1}{r^3}\,d\tau$$

and $X=\Delta E_3/\gamma_{ln}$, $\epsilon=\Delta E/\gamma_{ln}$, where ΔE_3 is the singlet-triplet separation.

[13] For details as to the reason for this, see S. Goudsmit, Phys. Rev. **31**, 956 (1928). For the case of (*jj*) coupling in the singlet-triplet case, see W. Pauli, Handbuch der Physik, vol. XXIII, pp. 254-257. The two pairs of levels ($^1P_1$ and $^3P_2$, $^3P_1$ and $^3P_0$) are expected to form a relativistic doublet.

We may note that the splitting-up of the multiplets ^3P and ^3D of the configuration $2s2p^3$ is, according to the approximation of Goudsmit, zero. One finds for the (*ii*) coupling case (1) for $j_1=1/2$, $j_2=1/2$, $j_3=1/2$, $j_4=3/2$ one state with $j=2$ and one with $j=1$, (2) for $j_1=1/2$, $j_2=1/2$, $j_3=3/2$, $j_4=3/2$ one state with $j=3$,one with $j=0$, and two each with $j=3$ and $j=1$, and (3) for $j_1=1/2$, $j_2=3/2$, $j_3=3/2$, $j_4=3/2$ one state with $j=2$ and one with $j=1$. The Γ value for $j=3$ is 0; for $j=2$, $\Sigma\Gamma=0$; for $j=1$, $\Sigma\Gamma=0$; and for $j=0$, $\Gamma=0$. This gives immediately the result of non-splitting. Actually, one observes a small splitting-up in O III, both triplets being resolved into two lines each. This is no doubt due to the presence of the other terms arising from the same electronic configuration. In C I, N II, and F IV, on the other hand, the triplets appear unresolved.

Also, choose as the functions of the unperturbed system the following:

$$\phi_1=(\tfrac{1}{2})\{P_0{}^0(1)P_l{}^m(2)+P_0{}^0(2)P_l{}^m(1)\}\{S_\alpha(1)S_\beta(2)-S_\alpha(2)S_\beta(1)\}$$
$$\phi_2=(\tfrac{1}{2})^{1/2}\{P_0{}^0(1)P_l{}^{m-1}(2)-P_0{}^0(2)P_l{}^{m-1}(1)\}S_\alpha(1)S_\alpha(2)$$
$$\phi_3=(\tfrac{1}{2})\{P_0{}^0(1)P_l{}^m(2)-P_0{}^0(2)P_l{}^m(1)\}\{S_\alpha(1)S_\beta(2)+S_\alpha(2)S_\beta(1)\}$$
$$\phi_4=(\tfrac{1}{2})^{1/2}\{P_0{}^0(1)P_l{}^{m+1}(2)-P_0{}^0(2)P_l{}^{m+1}(1)\}S_\beta(1)S_\beta(2).$$

With no magnetic field, the secular equation is

$$\begin{vmatrix} X-\epsilon & \tau & -m & -\tau' \\ \tau & m-1-\epsilon & \tau & 0 \\ -m & \tau & -\epsilon & \tau' \\ -\tau' & 0 & \tau' & -m-1-\epsilon \end{vmatrix}=0$$

Here

$$\tau=(\tfrac{1}{2})^{1/2}(l+m)^{1/2}(l-m+1)^{1/2}$$

and

$$\tau'=(\tfrac{1}{2})^{1/2}(l-m)^{1/2}(l+m+1)^{1/2}.$$

When the triplet and singlet can be handled separately, the energy values are:

$$\epsilon_{\mathrm{I}}=X, \qquad \epsilon_{\mathrm{II}}=l, \qquad \epsilon_{\mathrm{III}}=-1, \qquad \epsilon_{\mathrm{IV}}=-l-1.$$

The wave functions are:

$$\psi_1=\phi_1$$
$$\psi_{\mathrm{II}}=\{1/(l+1)(2l+1)\}^{1/2}[(\tfrac{1}{2})^{1/2}\{(l+m)(l+m+1)\}^{1/2}\phi_2 + \{(l-m+1)(l+m+1)\}^{1/2}\phi_3+(\tfrac{1}{2})^{1/2}\{(l-m)(l-m+1)\}^{1/2}\phi_4]$$
$$\psi_3=\{1/l(l+1)\}^{1/2}[-(\tfrac{1}{2})^{1/2}\{(l+m)(l-m+1)\}^{1/2}\phi_2+m\phi_3 + (\tfrac{1}{2})^{1/2}\{(l-m)(l+m+1)\}^{1/2}\phi_4]$$
$$\psi_{\mathrm{IV}}=\{1/l(l+1)\}^{1/2}[(\tfrac{1}{2})^{1/2}\{(l-m)(l-m+1)\}^{1/2}\phi_2-(l^2-m^2)^{1/2}\phi_3 + (\tfrac{1}{2})^{1/2}\{(l+m)(l+m+1)\}^{1/2}\phi_4].$$

Applying our previous method, we then solve the secular equation ($j=l$)

$$\begin{array}{c} \\ \psi_3 \\ \psi_1 \end{array}\begin{vmatrix} \psi_3 & \psi_1 \\ -1-\epsilon & -(l^2+l)^{1/2} \\ -(l^2+l)^{1/2} & X-\epsilon \end{vmatrix}=0$$

This results in

$$\psi_{\mathrm{I}}=(1/c_{\mathrm{I}}\Delta_l)^{1/2}\{c_{\mathrm{I}}\psi_1-(l^2+l)^{1/2}\psi_3\}$$
$$\psi_{\mathrm{III}}=(1/c_{\mathrm{III}}\Delta_l)^{1/2}\{c_{\mathrm{III}}\psi_1+(l^2+l)^{1/2}\psi_3\}$$

where

$$c_{\mathrm{I}}=\left|1+\epsilon_{\mathrm{I}}\right| \text{ and } c_{\mathrm{III}}=\left|1+\epsilon_{\mathrm{III}}\right| \cdot c_{\mathrm{I}}c_{\mathrm{III}}=l^2+l.$$

When X is large, $c_{\mathrm{I}} \cong \Delta_1$

For the $2p\ 3s$ configuration, the wave functions $\psi_{\mathrm{I}}, \psi_{\mathrm{II}}, \psi_{\mathrm{III}}, \psi_{\mathrm{IV}}$ are then used, with $l=1$, to find the matrix elements.

2. *The Triplet Separations.* For O III,

$$^1S_0-{}^3P:\Delta\nu \cong 43130$$
$$^1D_2-{}^3P:\Delta\nu \cong 20120.$$

It is at once seen that the ratio of separation 2:3 as derived from a first order perturbation calculation[10] is not in agreement with experiment, perhaps due to second order effects. We shall use the experimental data for what follows.

$$^3P_2-{}^3P_1:\Delta\nu=193$$
$$^3P_1-{}^3P_0:\Delta\nu=116.$$

Then

$$\epsilon_3=\frac{1}{2}[Y_1+1-\{(Y_1-1)^2+8\}^{1/2}]=\frac{1}{2}\left[2-\frac{4(Y_1+1)}{(Y_1-1)^2}\right]$$

$$\cong 1-\frac{2}{Y_1-3} \text{ so that } c_3 \cong \frac{2}{Y_1-3}.$$

Likewise,

$$c_1 \cong \frac{8}{Y_2-6}, \qquad \epsilon_1 \cong -2-\frac{8}{Y_2-6}.$$

If we assume

$$Y=100 \quad (\cong 309/3),$$

then

$$Y_2=431, \quad Y_1=201$$

and

$$\epsilon_3=0.99, \quad \epsilon_1=-2.02$$

The separation ratio is then 102:199, in much worse agreement with experiment than the results of Gaunt. It should be noted that the calculation here neglects the interaction between each electron and the orbit of the other, and also the magnetic interaction between the two electron spins.

For N II,

$$^1S_0-{}^3P:\Delta\nu \cong 32670\ ; \quad ^3P_2-{}^3P_1=83$$
$$^1D_2-{}^3P:\Delta\nu \cong 15300\ ; \quad ^3P_1-{}^3P_0=50$$

assuming[14]

$$\nu \cong 206160 \quad \text{for} \quad {}^1S_0.$$

If we take $\gamma=45(\cong 133/3)$, then $Y_2=726$, $Y_1=340$ and $\epsilon_3=.99, \epsilon_1=-2.01$. Here the separation ratio is 101:199.

[14] Reference 1, p. 65.

3. *The Matrix Amplitudes.* When one calculates integrals such as $\int\bar{\phi}_1 v\psi_\epsilon{}^2 d\tau$ the only ones that do not vanish are as in this case, where ϕ_1 and $\psi_\epsilon{}^2$ have the same spin factor. We abbreviate as follows: $v(\psi_\epsilon{}^2)=\int\bar{\phi}_1 v\psi_\epsilon{}^2 d\tau$, etc., and $z(\psi_\epsilon{}^2)=\int\bar{\psi}_\epsilon{}^2 z\phi_1 d\tau$. Further let $a=\int\overline{P_0{}^0}vP_1{}^{-1}d\tau$ and $b=\int\overline{P_1{}^0}zP_0{}^0 d\tau$. A list of integrals needed in the further calculation is given below.

$$v(\psi_\epsilon{}^2)=0 \quad v(\psi_\delta{}^1)=0 \quad v(\psi_\delta{}^0)=a \quad v(\psi_\epsilon{}^0)=0 \quad v(\psi_\delta{}^{-1})=a \quad v(\psi_\epsilon{}^{-2})=a2^{1/2}$$
$$v(\psi_\alpha{}^2)=0 \quad v(\psi_\alpha{}^1)=a \quad v(\psi_\alpha{}^0)=0 \quad v(\psi_\beta{}^0)=-a \quad v(\psi_\alpha{}^{-1})=a \quad v(\psi_\alpha{}^{-2})=-a$$
$$v(\psi_\gamma{}^1)=0 \quad v(\psi_\gamma{}^0)=a \quad v(\psi_\gamma{}^{-1})=-a \quad v(\psi_{\mathrm{IV}}{}^0)=a/3^{1/2} \quad v(\psi_{\mathrm{V}}{}^0)=-a2^{1/2}/3^{1/2}$$
$$z(\psi_\epsilon{}^2)=0 \quad z(\psi_\delta{}^1)=b \quad z(\psi_\delta{}^0)=0 \quad z(\psi_\epsilon{}^0)=b2^{1/2} \quad z(\psi_\delta{}^{-1})=b \quad z(\psi_\epsilon{}^{-2})=0$$
$$z(\psi_\alpha{}^2)=b \quad z(\psi_\alpha{}^1)=0 \quad z(\psi_\alpha{}^0)=b \quad z(\psi_\beta{}^0)=b \quad z(\psi_\alpha{}^{-1})=0 \quad z(\psi_\alpha{}^{-2})=b$$
$$z(\psi_\gamma{}^1)=b \quad z(\psi_\gamma{}^0)=0 \quad z(\psi_\gamma{}^{-1})=b \quad z(\psi_{\mathrm{IV}}{}^0)=2b/3^{1/2} \quad z(\psi_{\mathrm{V}}{}^0)=b2^{1/2}/3^{1/2}.$$

One readily verifies the Laporte rule for dipole radiation for $^1D\rightarrow{}^3P$.

The matrix components which we need follow.

$$^1D_2\rightarrow{}^1P_1: \quad z(m,m)=\frac{b(1+c_4c_{\mathrm{I}})}{(c_{\mathrm{I}}\Delta_1c_4\Delta_2)^{1/2}}\cdot\left(\frac{4-m^2}{3}\right)^{1/2}$$

$$^1D_2\rightarrow{}^3P_2': \quad z(m,m)=-\frac{b}{(c_4\Delta_2)^{1/2}}\cdot\frac{m}{2^{1/2}}$$

$$^1D_2\rightarrow{}^3P_1': \quad z(m,m)=\frac{b(-1+c_4c_{\mathrm{III}})}{(c_{\mathrm{III}}\Delta_1c_4\Delta_2)^{1/2}}\cdot\left(\frac{4-m^2}{3}\right)^{1/2}$$

$$^1P_1\rightarrow{}^3P_2: \quad v(m,m-1)=\frac{a(1+c_1c_3)}{(c_{\mathrm{I}}\Delta_1c_3\Delta_2)^{1/2}}\cdot\left(\frac{1}{6}\right)^{1/2}[(3-m)(2-m)]^{1/2}$$

$$^1P_1\rightarrow{}^3P_1: \quad v(m,m-1)=\frac{a}{2(c_{\mathrm{I}}\Delta_1)^{1/2}}[(1+m)(2-m)]^{1/2}$$

$$^1P_1\rightarrow{}^3P_0: \quad v(m,m-1)=\frac{a}{(c_{\mathrm{I}}\Delta_1c_1\Delta_0)^{1/2}}(2/3)^{1/2}(4+c_1c_{\mathrm{I}}) \qquad (m=1)$$

$$^3P_2'\rightarrow{}^3P_2: \quad v(m,m-1)=\frac{a}{2(c_3\Delta_2)^{1/2}}[(2+m)(3-m)]^{1/2}$$

$$^3P_2'\rightarrow{}^3P_1: \quad v(m,m-1)=-\frac{a}{2(6)^{1/2}}[(2+m)(1+m)]^{1/2}$$

$$^3P_1'\rightarrow{}^3P_2: \quad v(m,m-1)=\frac{a(1-c_3c_{\mathrm{III}})}{(c_{\mathrm{III}}\Delta_1c_3\Delta_2)^{1/2}}\left(\frac{1}{6}\right)^{1/2}[(3-m)(2-m)]^{1/2}$$

$$^3P_1'\rightarrow{}^3P_1: \quad v(m,m-1)=\frac{a}{2(c_{\mathrm{III}}\Delta_1)^{1/2}}[(1+m)(2-m)]^{1/2}$$

$$^3P_1'\rightarrow{}^3P_0: \quad v(1,0)=\frac{a}{(c_{\mathrm{III}}\Delta_1c_1\Delta_0)^{1/2}}\left(\frac{2}{3}\right)^{1/2}(-4+c_1c_{\mathrm{III}}).$$

It is seen, on going to the limit of non-intercombination, that these matrix elements are precisely equivalent to those ordinarily used, as for instance corresponding to the formulae given at the beginning of this paper. This is a useful check on the correctness of the calculation. Another check would be to go to the limit of (*jj*) coupling, but, to the writer's knowledge, the intensities have not been worked out for this case. Granted that this probem had been solved, however, it might be possible, without going through our perturbation calculation, to derive the necessary matrix components by a process of interpolation between the two limiting cases. This method should be particularly advantageous in treating the $2s2p^3$ configuration, where the wave functions appear in the form of determinants[15] with four rows and columns, and where, by a straightforward method such as used here, one would need to solve two secular equations of the fourth degree, for $j=2$ and for $j=1$, respectively.

4. *The Intensities (Amplitudes Squared) and the Summation Rule.* In Table III, the squared amplitudes for the transitions of $2p3s-2p^2$ are given,

TABLE III. *Intensities for* $2p3s-2p^2$.

	$^1P_1$	$^3P_2$	$^3P_1$	$^3P_0$	Sum	Limit of sum
$^1S_0$	$\frac{2}{c_5\Delta_0}\ \frac{\{c_1c_5-4\}^2}{c_1\Delta_1}$		$\frac{2}{c_5\Delta_0}\ \frac{\{c_{III}c_5+4\}^2}{c_{III}\Delta_1}$		2	2
$^1D_2$	$\frac{10}{c_4\Delta_2}\ \frac{\{1+c_4c_1\}^2}{c_1\Delta_1}$	$\frac{15}{c_4\Delta_2}$	$\frac{10}{c_4\Delta_2}\ \frac{\{c_4c_{III}-1\}^2}{c_{III}\Delta_1}$		10	10
$^3P_2$	$\frac{10}{c_3\Delta_2}\ \frac{\{c_3c_1-1\}^2}{c_1\Delta_1}$	$\frac{15}{c_3\Delta_2}$	$\frac{10}{c_3\Delta_2}\ \frac{\{1+c_3c_{III}\}^2}{c_{III}\Delta_1}$		10	10
$^3P_1$	$\frac{3}{c_1\Delta_1}$	$\frac{5}{2}$	$\frac{3}{c_{III}\Delta_1}$	2	6	6
$^3P_0$	$\frac{2}{c_1\Delta_0}\ \frac{\{c_1c_1+4\}^2}{c_1\Delta_1}$		$\frac{2}{c_1\Delta_0}\ \frac{\{4-c_1c_{III}\}^2}{c_{III}\Delta_1}$		2	2
Sum	$\frac{12(c_1^2+1)}{c_1\Delta_1}$	10	$\frac{12(c_{III}^2+1)}{c_{III}\Delta_1}$	2	30	
Limit of sum	12	10	6	2		30

together with sums from a given upper level or a given lower level. To calculate the sums, we use relations such as $c_1+c_5=\Delta_0$, $c_5^2+8=c_5\Delta_0$, etc. The limit of the sum, as the electrostatic interaction between the electrons is increased, is also given. In general, these limits are proportional to the statistical weights of the corresponding levels, excepting when $^1P_1$ is the upper level, where the limit is twice as much, probably due to the existence of two lower levels (^1S and ^1D) of the same multiplicity. (The $2p3s$ ^3P level may, in the limit, only combine with the one level $(2p)^2$ ^3P.

[15] See J. C. Slater, Phys. Rev. (being published). The separations between multiplets of the $2s2p^3$ configuration, as well as of $2p^2$ are in fair agreement with theoretical expectations although there is probably a mutual disturbance, giving a second-order correction. I am indebted to Professor Slater for the privilege of seeing the manuscript before publication.

III. Quadrupole radiation for intercombinations between states of different multiplicities

As before, we shall calculate for extreme cases, and suppose the actual relations of intensities to correspond to an intermediate case.

Case 1. ^1P the intermediate state.

a. $^1D_2 \rightarrow {}^3P_2$ $$[zv](m,m-1)=\frac{ab(1+c_4c_1)(1+c_3c_1)(2-m)\{(2+m)(3-m)\}^{1/2}}{\Delta_2c_1\Delta_1(18c_3c_4)^{1/2}}$$

$$\sum(zv)^2=\frac{11a^2b^2(1+c_4c_1)^2(1+c_3c_1)^2}{3c_1^2c_3c_4\Delta_1^2\Delta_2^2}$$

b. $^1D_2 \rightarrow {}^3P_1$ $$[zv](m,m-1)=\frac{ab(1+c_4c_1)(2-m)\{(2+m)(1+m)\}^{1/2}}{c_1\Delta_1(12c_4\Delta_2)^{1/2}}$$

$$\sum(zv)^2=\frac{7a^2b^2(1+c_4c_1)^2}{6c_1^2\Delta_1^2c_4\Delta_2}$$

c. $^1D_2 \rightarrow {}^3P_0$ $$\{[zv](1,0)\}^2=\frac{2a^2b^2(1+c_4c_1)^2(4+c_1c_1)^2}{3c_1^2c_1c_4\Delta_0\Delta_1^2\Delta_2}$$

For O III,

$$c_1 \leqq \Delta_1=45.6,\ c_1 \leqq \frac{8}{Y_2-6}=\frac{8}{425} \text{ and } c_3 \leqq \frac{2}{Y_1-3}=\frac{2}{198}.$$

The relative intensities are then $a:b:c=3.9:1.2:1.9$

For N II,

$$c_1 \leqq 4,\ c_1 \leqq \frac{8}{720},\ \text{and}\ c_3 \leqq \frac{2}{337}.$$

Here the relative intensities are $a:b:c=1.9:1.2:1.4$

Case 2. $^3P_2'$ the intermediate state.

a. $^1D_2 \rightarrow {}^3P_2'$ $$[zv](m,m-1)=-\frac{abm\{(2+m)(3-m)\}^{1/2}}{\Delta_2(8c_3c_4)^{1/2}}$$

$$\sum(zv)^2=\frac{13a^2b^2}{4\Delta_2^2c_3c_4}$$

b. $^1D_2 \rightarrow {}^3P_1$ $$[zv](m,m-1)=\frac{abm\{(2+m)(1+m)\}^{1/2}}{4\cdot 3^{1/2}(c_4\Delta_2)^{1/2}}$$

$$\sum(zv)^2=\frac{25a^2b^2}{24c_4\Delta_2}.$$

The relative intensities are $a:b=39:25$. $c=0$

Case 3. $^3P'_1$ the intermediate state.

$$a.\ {}^1D_2\rightarrow{}^3P_2 \quad [zv](m,m-1)=\frac{ab(-1+c_4c_{III})(1-c_3c_{III})(2-m)\{(2+m)(3-m)\}^{1/2}}{c_{III}\Delta_1\Delta_2(18c_3c_4)^{1/2}}$$

$$\sum(zv)^2\leqq\frac{11a^2b^2(-1+c_4c_{III})^2}{3c_{III}^2c_3c_4\Delta_1^2\Delta_2^2}$$

$$b.\ {}^1D_2\rightarrow{}^3P_1 \qquad \sum(zv)^2=\frac{7}{6}\ \frac{a^2b^2(-1+c_4c_{III})^2}{c_{III}^2\Delta_1^2c_4\Delta_2}$$

$$c.\ {}^1D_2\rightarrow{}^3P_0 \qquad \{[zv](10)\}^2=\frac{32}{3}\ \frac{a^2b^2(-1+c_4c_{III})^2}{c_{III}^2\Delta_1^2c_1\Delta_0c_4\Delta_2}$$

The relative intensities in this case are $a:b:c=11:7:8$.
The experimental data indicates that the relative intensities should be approximately $a:b:c=2:1:0$.

Discussion

The purpose of this paper has been to test the idea that quadrupole radiation is the important factor in causing the nebular lines (forbidden for dipole radiation) to be emitted. One result stands forth quite clearly, namely, that, with such an assumption, the line of a multiplet which should theoretically be strongest, is in fact such according to the experiments. We obtain a disagreement, however, when the relative intensities of the weaker line are considered. This may be because of the simplifications and approximations made during the course of the calculations.

It is a pleasure to acknowledge my indebtedness to Professor W. Pauli, both for permission to study at his institute, and for his clarifying and illuminating remarks. It is also a privilege to thank Harvard University for the award of a Parker Travelling Fellowship, without which study in Europe would have been impossible.

ON METHODS OF FILTER RADIOMETRY

By Donald C. Stockbarger and Laurence Burns
Massachusetts Institute of Technology

(Received September 14, 1929)

Abstract

The principal error in filter radiometry is analyzed and shown to be due to interpretation of results rather than to the sloping transmission characteristics of the radiation filters which make the boundaries of the spectral regions appear to be indefinite. It is shown that if the filter cut-off is assumed to be at the point where the transmission of the filter becomes zero, as is done in many instances, the observed radiant power of the spectral band so defined is in error, but that the error can be made to disappear by assuming the cut-off to be at a different wave-length.

This effective cut-off of a filter is located at such a wave-length that the energy transmitted by the filter below, is equal to that which is selectively absorbed by it above the cut-off. In effect the transmission curve of the filter is thus changed to one of rectangular shape so that it cuts off sharply at the effective wave-length.

Two simple analyses of water-filtered quartz mercury arc radiation were made with the aid of two glass filters. The zero percent cut-off of the first coincided with the effective cut-off of the second, so that a comparison could be made between the two interpretations. A very considerable difference was found between the results when the usual approximate correction factor was applied to the first result, but by substituting the exact factor, computed from line intensity measurements, the results of the two analyses were made to agree within about one-half of one percent. This indicated the usefulness of the effective cut-off method in making accurate radiation measurements.

THE quantitative analysis of radiation consists in measuring the powers or intensities of radiant energy within specified spectral regions. The energy measurements are made preferably by means of a non-selective, quantitative detector such as the thermopile. The simplest and perhaps most commonly employed device for separating spectral regions is the radiation filter, e.g., crown glass. Due to the indefiniteness of the transmission cut-offs of practical filters the results obtained are in general only roughly of the right order of magnitude; they may even be meaningless. Theoretically, filters should have transmission curves of rectangular shape so that the cut-offs would be abrupt instead of gradual. A somewhat analogous situation exists in the sifting of sand by means of a wire screen the mesh of which is not uniform. If the sand were thrown against such a screen placed in an inclined position, the quantity of sand accumulating beneath the screen would not furnish definite information as to the proportion of material having a particle size less than the size of the smallest screen opening. In order to interpret the results it would be necessary to apply a correction factor based on the composition of the sand and on the relative numbers of screen openings of each size. Similarly in filter radiometry the observed energies need to be corrected before the numerical values can be interpreted.

Although some care can be exercised in the selection of filters so as to avoid excessively sloping cut-offs, nothing can be done to change their poor characteristics and therefore attention must be focused on the interpretation of the results obtained by their use. This paper is intended to show that through correct interpretation accurate figures are obtainable.

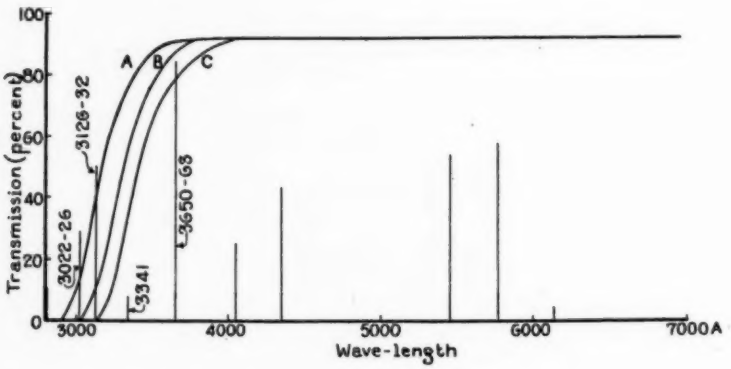

Fig. 1. Spectral transmission curves of "neutral" glasses.
The vertical lines represent mercury arc lines.

A common interpretation is that the cut-off of a filter is at the wavelength where its transmission becomes zero. This may lead to ridiculous conclusions particularly when the energy of a narrow spectral region is being determined as the difference between the energies of two wide bands one of which includes the region in question. For example, referring to Fig. 1 and

TABLE I. *Intensities of water-filtered quartz mercury arc lines and groups. I_0 is the original intensity; I_a the intensity after transmission by one A filter; I_{aa} the intensity after transmission by two A filters; etc.*

Wave-length	I_0	I_a	I_{aa}	I_b	I_{bb}
3022–26	5.8	0.8	0.1	0.0	0.0
3126–32	10.0	4.1	1.7	1.1	0.1
3341	1.5	1.2	0.9	0.9	0.5
3650–63	16.9	15.4	14.0	14.7	12.8
4047	5.1	4.7	4.3	4.7	4.3
4339–58	8.6	7.9	7.3	7.9	7.3
5461	10.9	10.0	9.2	10.0	9.2
5770–90	11.8	10.9	10.0	10.9	10.0
6123–6234	0.9	0.8	0.8	0.8	0.8
10140	3.0	2.8	2.5	2.8	2.5
11287	1.4	1.3	1.2	1.3	1.2
Total for *A*	75.9	59.9	52.0		
Total for *B*	70.1			55.1	48.7

Table I, filters *A* and *B* might be selected for measuring the intensity of the 3022–26A mercury group, for the former transmits the lines to a certain extent whereas the latter does not. From the tabulated data it is readily

shown that the observed intensity would be 4.8 as compared with the true value 5.8. The first figure is not greatly different from 4.0 which would be obtained if the two lines were absent and therefore cannot be closely related to the wanted intensity.

To obtain correct figures it is necessary to correct both galvanometer readings for the absorption losses of the corresponding filters. The first galvanometer reading is proportional to the rate at which energy falls on the receiving surface of the thermopile through filter A. Another way of stating it is that the reading is proportional to the sum of the intensities of the lines, transmitted by the filter, after transmission. What the observer really wishes to know is the sum of the intensities before transmission. Symbolically he is trying to measure ΣI_0 where I_0 is the original intensity of any line and where Σ represents the summation over the spectral region in which the filter is able to transmit any energy. Actually he measures ΣI_a which differs from ΣI_0 only in that I_a equals I_0 multiplied by the transmission of the filter at the wave-length of the line whose intensity is I_0. The ratio $\Sigma I_a/\Sigma I_0$ is the average correction factor for the spectral region lying between the limits of filter A, and is the quantity by which the first galvanometer reading should be divided. It may be called the "true filter factor." Similarly, the second galvanometer reading, made with filter B covering the thermopile, should be divided by $\Sigma I_b/\Sigma I_0$, the summations now being made over the spectral band between the transmission limits of B. If in the example of the preceding paragraph each of the two observed band intensities had been divided by the respective true filter factor the difference between the corrected values would have been the actual intensity of the 3022-26A group.

The difficulty of the method is that in order to obtain the correct filter factor, which is but a step toward the solution, ΣI_0 must be known. ΣI_0 is the solution itself. As a rough approximation the filter factor is often determined[1,2] experimentally by dividing the intensity of the radiation which has been transmitted successively through two identical filters by that of the radiation which has been transmitted by one of the two filters. In other words the spectral region is isolated by the first filter, so that the fractional part of the energy in that region passing through the second can be measured. An error is introduced by the alteration of energy distribution in the band due to the selective transmission of the first filter near the band limits, i.e., departure from rectangular shape of the transmission curve. Analytically, the experimentally determined filter factor is the ratio of ΣI_{aa} to ΣI_a, where I_{aa} is the intensity of a spectral line after passing successively through two A filters. Making the summations indicated above for both filters we obtain:

$$\frac{\Sigma I_a \times \Sigma I_a}{\Sigma I_{aa}} = \frac{59.9 \times 59.9}{52.0} = 69.0$$

[1] Coblentz, Long and Kahler, Bur. Stds. Sci. Paper, No. 330, Page 17.
[2] Stockbarger, J.O.S.A. & R.S.I. **14**, 359 (1927).

$$\frac{\Sigma I_b \times \Sigma I_b}{\Sigma I_{bb}} = \frac{55.1 \times 55.1}{48.7} = 62.4.$$

While it is evident that the two corrected band intensities are in error, they are more nearly correct than the measured intensities. This partial elimination of errors has doubtless saved many a piece of work from being entirely worthless, but in the particular example discussed above it has not helped much in the determination of the intensity of the 3022–26A group for again the difference would not be zero if the group were absent. The difficulty is increased in the present case by the close proximity of the 3126–32A group which is transmitted by the *A* filter nearly four times as well as by the *B* filter. When the band measured by difference is wide, so that a considerable part of it lies under the flat part of the transmission curve of the *A* filter, the relative error in the difference is not nearly as great as found above. Moreover, if in addition to measuring wide bands, the filters are so chosen that their regions of lowest transmission coincide with the regions

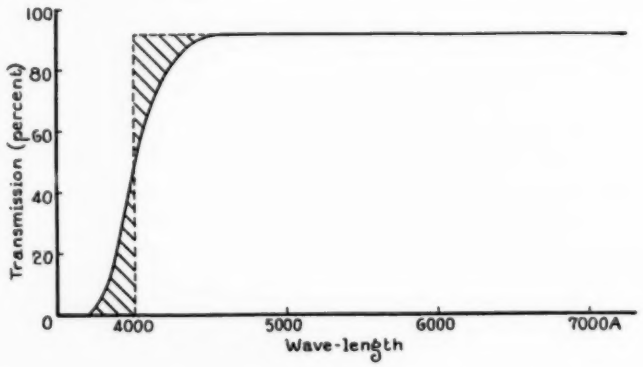

Fig. 2. Location of the effective cut-off of filter for an equal energy spectrum.

containing relatively few lines of importance, the errors due to departure from rectangular transmission curves are still further reduced.

Referring to Fig. 2 it is at once apparent that for an equal energy spectrum the effective cut-off of a filter can be located at such a wave-length that the equivalent of a rectangular transmission curve results. The energy which is transmitted by the filter below the cut-off equals that which is selectively absorbed above it. The correction factor for such a filter is evidently the maximum transmission value. While in practice equal energy spectra are not met, the principle can be applied to any spectrum whose energy distribution is known in the region of poor transmission. By a proper choice of the effective cut-off wave-length, the error resulting from discarding transmitted energy below, is made to balance the error on the other side due to departure from rectangular transmission characteristics. When employed in this manner the filter yields the same results in analytical work as would a truly ideal one, and its factor has the same value as its maximum trans-

mission. This equivalent rectangular transmission curve concept is particularly valuable in that it eliminates at once the greatest source of error inherent in the older method, viz., the approximate filter factor.

Besides the spectral transmission characteristics of the filter, which would be known in any case, it is necessary to know the energy distribution of the source in the region of poor transmission only. Ordinarily approximate distribution values suffice, for the strongest lines determine largely the location of the effective limit; sometimes the latter can be estimated by inspection of a spectrogram. If the cut-off should fall within a narrow region of high energy content, such as the 3650–63A mercury group, a filter of different thickness or composition should be selected so as to shift it above or below as desired.

To make a direct comparison between the two methods two simple radiation analyses of water-filtered quartz mercury arc radiation were made with the aid of a suitable thermopile and galvanometer. Each of these analyses consisted in determining the intensity of that part of the radiation which lay

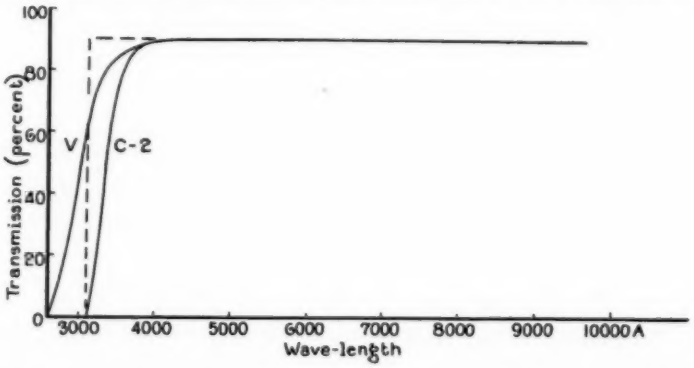

Fig. 3. Spectral transmission curves of the two filters employed to determine the intensity of water-filtered quartz mercury arc radiation of wave-lengths longer than 3100A.

on the long wave-length side of 3100A. The water filtering was done by means of a one centimeter quartz water cell, the purpose being to insure that the long wave-length limit of the spectral region was the same in both cases. This use of the quartz water cell is standard practice and is generally necessary for the infra-red limits of the glass filters are far from identical. The first analysis by the old zero cut-off method was made by means of filter *C-2* whose spectral transmission characteristics are shown in Fig. 3. The effective cut-off of the *V* filter employed in the second analysis was at the same wave-length as the zero cut-off of the *C-2* filter, i.e., 3100A as indicated by the vertical broken line in the figure. It is of interest to note that the transmission of the *V* filter is approximately 60 percent at this point. The method employed to determine the effective cut-off of this filter is made evident in Table II, which gives also the relative intensities of the important mercury lines and groups after transmission by the water cell. The operating conditions of the arc including current and arc voltage, which obtained when the line intensities were measured, were duplicated closely during the analyses.

The observed filter factor for *C2* was 0.872. As a check on the reliability of the intensity data it is of interest to compute the factor by dividing $\Sigma I_{(c_2)^2}$ by ΣI_{c_2}, taking the values from Table II. The ratio thus obtained, 0.868, is in good agreement with the observed value indicating that it is safe to compute the true filter factor in a similar manner. This is accomplished by dividing ΣI_{c_2} by ΣI_0, the latter summation being made over the transmitted spectral band as indicated in the same table. The quotient is 0.756. Compare this with 0.872 which was observed by the approximate method.

In the first analysis the ratio of galvanometer deflections with and without *C-2* was 0.571. Dividing this by the true filter factor, 0.756, the corrected ratio is found to be 0.755, which is the figure sought in the analysis. Were the approximate filter factor used the figure would be 0.655.

TABLE II. *Relative intensities of water-filtered quartz mercury arc lines and groups. I_0 is the original intensity; I_v, the intensity after transmission by filter V; $I(C_2)^2$, the intensity after transmission by two C-2 filters; etc.*

Wave-length	I_0	$0.904I_0$	I_v	$0.904I_0-I_v$	IC_2	$I(C_2)^2$
2537	4.7	4.2	0.0	4.2	0.0	0.0
2652	4.6	4.2	0.2	4.0	0.0	0.0
2804	2.1	1.9	0.4	1.5	0.0	0.0
3022–26	5.8	5.2	2.9	2.3	0.0	0.0
3126–32	10.0	9.0	6.4	2.6	0.4	0.0
3341	1.5	1.4	1.2	0.2	0.8	0.4
3650–63	16.9	15.3	14.6	0.7	14.2	11.9
4047	5.1	4.6	4.5	0.1	4.6	4.1
4339–58	8.6	7.8	7.7	0.1	7.7	6.9
5461	10.9 *	9.9	9.9	0.0 *	9.9	8.9
5770–90	11.8	10.7	10.7	0.0	10.6	9.6
6123–6234	0.9	0.8	0.8	0.0	0.8	0.7
10140	3.0	2.7	2.7	0.0	2.7	2.4
11287	1.4	1.3	1.3	0.0	1.3	1.1
Total	*70.1		*3.5	*3.7	53.0	46.0

* Total as indicated.

In the second analysis the ratio of galvanometer deflections with and without *V* was 0.685. Dividing by the factor 0.904, the maximum transmission of the filter, the value 0.758 is obtained. The agreement with 0.755 found in the first analysis is all that could be desired, and it indicates clearly the usefulness of the effective cut-off method of analyzing radiation.

The source of radiation used in the above analyses was a combination of mercury arc and water cell. Therefore its long wave-length limit was approximately 14,000A.[3] If, however, the water cell had not been a part of the source but had been included in the analyzing system, so that band intensities were referred to total bare source radiation, the procedure would have been somewhat different.

In either example the corrected ratio would have been multiplied by the ratio of galvanometer deflections with and without the water cell cover-

[3] Aschkinass, Ann. d. Physik 55, 401 (1895).

ing the thermopile. The latter ratio would have been corrected by dividing by the filter factor or by the maximum cell transmission, depending upon whether the old or the new method, respectively, had been adopted. The results by the two methods would not have been identical for the long wave-length limits of the regions would have been 14,000A and 11,000A, respectively. The latter was the effective cut-off of the water cell under the conditions of the analysis. Viewing the subject from another angle, the intensity of the water-cell-filtered quartz mercury arc radiation lying in the region 3100–14,000A was 0.9 the intensity of the unfiltered arc radiation lying in the band 3100–11,000A. Therefore the latter intensity could have been obtained by dividing the former by 0.9. If, however, the former had been divided by the true water-cell factor, a quantity smaller than the maximum transmission, the corrected intensity would have been that of the unfiltered band 3100–14,000A. The increase in value over that for the unfiltered 3100–11,000A band would have compensated exactly for the shifting of the long wave-length limit.

The question naturally arises as to how the calculations should be made in practice when a quartz water cell is used as an analyzing filter. For the greatest accuracy, provided that the energy distribution in the neighborhood of the boundary is known, the effective cut-off method should be used. From the standpoint of cost and convenience, however, the old method has the advantage that a pair of identical cells can be used for all work. The new method requires an adjustable cell or a number of cells of fixed depths so that the boundaries for different sources can be made to coincide. A standard solution which could be diluted to any desired strength might be used in work in which the absorption by the solute would not interfere with measurements in the ultra-violet. Adjustable cells are likely to prove unsatisfactory because of contamination of the water. Experience has demonstrated that fused quartz cells fabricated without the use of cement or other soluble material and fitted with ground quartz stoppers are the most reliable.

If the source is known to be rich in radiation in the region of the lower cut-off of the water cell, the short wave-length limit of the latter should be considered also. Paucity of data on the energy distribution in this region often makes it difficult to estimate the wave-length of the effective cut-off. Furthermore, the energy which is of wave-lengths shorter than the lower effective limit of the water cell is added to that of wave-lengths longer than the upper effective limit, so that while the contribution to the infra-red may be relatively small the error introduced in the far ultra-violet region may be considerable. If the source is not rich in this region, however, the quantity reported as far ultra-violet should be very nearly correct.

Summarizing, spectral bands can be isolated for purposes of radiometry by means of filters, but due to inherent characteristics of the latter the boundaries are not sharp enough to permit precise measurements. It is possible to compensate for the errors by correcting the observed quantities by means of filter factors, but the factors themselves are not readily determined

with accuracy. Only when the true filter factors are used are the results of the analyses correct. Adopting the viewpoint that the effective spectral limit of a filter is not at the point where the transmission curve touches the zero line, but at a point further up the curve, the filter can be made to behave as though its transmission curve were rectangular. This makes it possible to dispense with the filter factor and permits the use of the maximum filter transmission in place of the factor in correcting observed intensities for filter losses.

Some knowledge of the energy distribution of the radiation must be had before the effective cut-off can be located. At first this may seem to be an objectionable feature of the new method, but it is to be remembered that the distribution need be known only in the region of poor filter transmission. On the other hand to employ the old zero cut-off method to advantage the energy distribution throughout the entire spectral region transmitted by the filter should be known. In case energy distribution data are not available, the positions of the effective cut-offs in the visible and ultra-violet regions can be estimated from spectrograms with an accuracy comparable with, or perhaps far exceeding, that of estimating filter factors.

Taking relative accuracy and ease of use into account the effective cut-off method appears to possess advantages which warrant its adoption whenever possible.

Acknowledgment is made to the Cooper Hewitt Electric Company for the loan of apparatus and to Mr. A. L. M. Dingee and Mr. L. B. Johnson for assistance in making several of the physical measurements.

PACKING OF HOMOGENEOUS SPHERES

By W. O. Smith, Paul D. Foote and P. F. Busang
Mellon Institute of Industrial Research*

(Received September 26, 1929)

Abstract

Although the actual packing of shot is of a very irregular and distorted pattern, for certain statistical purposes the arrangement may be treated as a mixture of close-hexagonal and simple-cubical pilings in the proportion required to yield the observed porosity. The average number of contacts per sphere was determined by a simple method for several porosities and was found to agree with the value computed on the above assumption. Statistical distribution curves for contact numbers are also included. For higher porosities the distribution is Gaussian in general character.

IN THE regular arrangements, uniform shot may be piled in close hexagonal array with the minimum porosity of 0.26, and in simple cubical array with the maximum porosity 0.48. Such ideal arrangements however are not often realized in practice. Ordinarily, shot pack to a porosity in the neighborhood of 0.40, but with special care the porosity may be varied over the range 0.35–0.45. The question naturally arises therefore as to the type of packing yielding observed porosities. A general regularity is found to be absent. In places the shot are packed in close hexagonal array and at a short distance from these points the arrangements may be cubical. The patterns are in general distorted and spheres are frequently missing with a consequent closing-in and bridging of the pore cell. An investigation of the average number of contacts per sphere appeared to offer possibilities for a statistical consideration of the problem.

Lead shot of radius 3.78 mm were poured into a large beaker and a 20 percent solution of acetic acid was slowly introduced from the bottom until the beaker was filled. The acid was then carefully drained and at each contact between grains a small ring of liquid is retained by capillarity. On standing several hours this forms basic lead acetate clearly indicating the contact by a white circular deposit. The contacts may be readily counted as the shot are individually removed from the beaker. From 1,200 to 2,400 shot were used in beakers of 8 to 13 cm diameter but the count of contacts was confined to the interior 900 to 1,600 shot in order to reduce the effect of boundary conditions. The mean porosity for the interior shot was determined in the following manner. The volume of a cylinder passing through the centers of the spheres adjacent to the side walls, and cut by planes through the centers of the top and bottom layers of spheres, was computed, and from this was subtracted the actual volume of the shot and portions of shot lying within the space, as determined by count. The ratio of this final quantity to the total volume of the space considered is the porosity P.

* Gulf Oil Companies' Multiple Industrial Fellowship.

Table I summarizes the experimental data. The third column gives the average number of contacts n per sphere for a given observed porosity and the succeeding columns show the statistical distribution. The distributions on a percentage basis are plotted in Fig. 1. The curves for the larger porosities resemble Gaussian distributions and a pronounced shift toward higher

TABLE I. *Summary of data.*

Counted shot	P	n	Distribution of contacts per sphere								
			4	5	6	7	8	9	10	11	12
1562	0.359	9.14	1	13	77	245	322	310	208	194	192
1494	.372	9.51	0	14	86	192	233	193	161	226	389
887	.426	8.06	0	14	69	182	316	212	87	7	0
906	.440	7.34	3	54	173	309	233	118	14	2	0
905	.447	6.92	6	78	243	328	200	48	2	0	0

contacts per sphere occurs as the porosity is decreased. For the lower porosities the closer packing throws more spheres into the hexagonal array thus increasing the number of 10–12 point contacts. Usually the various porosities were obtained by shaking and tapping the beaker but for curves A and B small amounts of shot were successively added and shaken, and for curve B the shot in addition were tamped with a piston. Under this mode of packing the porosity in general decreases considerably with depth while the number

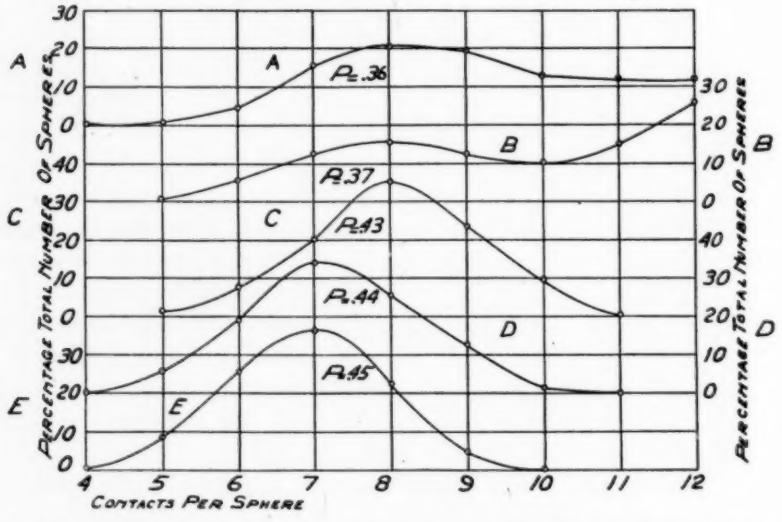

Fig. 1. Distribution of number of contacts per sphere for several porosities.

of contacts per sphere correspondingly increases. These variations however were carefully investigated and found consistent with the variation of the average number of contacts and the average porosity for the entire group of interior shot; hence it has not been necessary to consider the various zones or layers of shot in further detail.

In Fig. 2 is plotted the average number of contacts per sphere as a function of the porosity. The closest packing possible is hexagonal giving a porosity of 0.2595 and 12 contacts per sphere. It is evident that any theoretical or empirical curve must pass through this point. The most open regular array is simple cubic with porosity 0.4764 and 6 contacts per sphere. It appears doubtful that the presence of bridging could produce higher porosity and lower average contacts per sphere over an extended volume, and confirmation of this statement is amply afforded by the experimental data.

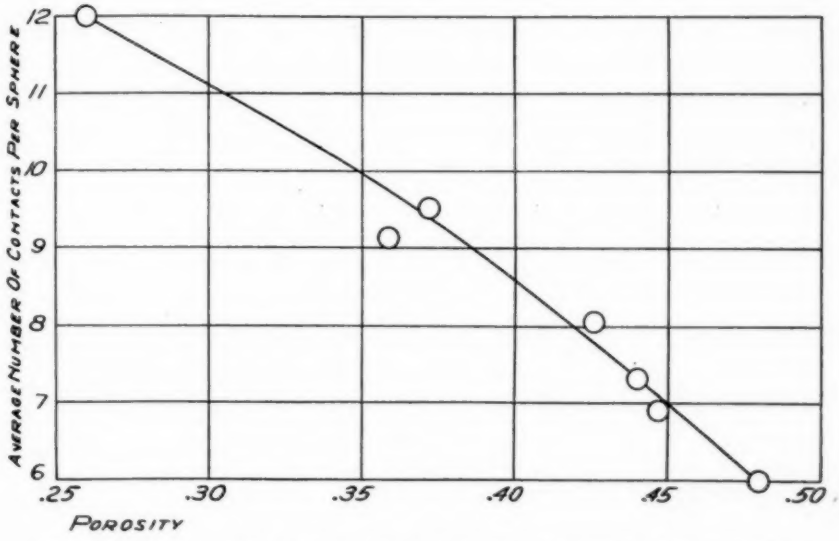

Fig. 2. Average number of contacts per sphere as a function of the porosity.

The fact therefore that the experimental results may be represented by a smooth curve through these two extreme points suggests the possibility of statistically treating the actual packing as an arrangement in separate hexagonal and cubical arrays in the proportion required to yield the observed porosity.

Let x be the fraction of the total volume of shot packed hexagonally $1-x$ the fraction packed cubically. Then

$$P=0.2595x+0.4764(1-x)$$

and

$$x=(0.476-P)/0.217. \tag{1}$$

In hexagonal array the number of spheres in unit volume is $2^{1/2}/8r^3$ and in cubical array $1/8r^3$. Hence for the mixture the average number of contacts per sphere is given by the relation

$$n=\frac{12x2^{1/2}/8r^3+6(1-x)/8r^3}{x2^{1/2}/8r^3+(1-x)/8r^3}=6\frac{1+1.828x}{1+0.414x}. \tag{2}$$

The quantity n as a function of P may be therefore obtained from Eqs. (1) and (2). The curve in Fig. 2 was drawn through points computed in the above manner and the agreement with experiment is surprisingly good. It is of interest that the regular body-centered piling with porosity 0.32 and 8 contacts per grain can not be correlated with the curve.

Especial theoretical significance should not be attached to the proposed interpretation of the packing problem. The complete solution must explain how shot acted upon by gravitational and frictional forces are arranged to give the contact distribution curves of Fig. 1. This problem presents extreme difficulty and its solution is not likely to be obtained in the near future. The present work however empirically demonstrates that when spheres are piled irregularly they may be statistically regarded as an arrangement in separate, close-hexagonal and simple-cubical arrays in a proportion to yield the observed porosity.

EFFECT OF TEMPERATURE UPON THE FLUORESCENCE OF SOME ORGANIC SOLUTIONS

By J. R. Jenness
Department of Physics, Cornell University

(Received August 2, 1929)

Abstract

A spectrographic study has been made of the effect of temperature upon the fluorescence of alcoholic solutions of rhodamine B, eosin, tetrachlorofluorescein, and sulfonefluorescein. Fluorescein has been studied by means of a spectrometer. The effect of concentration has been studied for eosin and for rhodamine B. When observed, the temperature shift of the peak of the fluorescence bands is proportional to the change in temperature. The observed change is in the same direction as has been observed for absorption. The shift is not in the same direction for all substances. The shift, due to change in concentration, is proportional to the logarithm of the concentration. The shift is in the same direction as it is for absorption. Change in the width of the fluorescence band does not follow the same law as for absorption. In other respects the results caused by change in temperature or change in concentration seem to be the same for absorption as for fluorescence.

Rhodamine B. Decrease in temperature or increase in concentration causes the peaks of the bands to shift to longer waves. Decrease in concentration causes a widening of the fluorescence band, but causes a narrowing of the absorption band.

Eosin. Decrease in temperature causes a shift to shorter waves for fluorescence peaks. This is probably true for absorption. Concentration shifts were too slight to be accurately measured. Fluorescence is a maximum at room temperature.

Fluorescein. Decrease in temperature causes a shift toward shorter waves. Fluorescence is a maximum at room temperature. Increase in temperature causes a widening of both the fluorescence and the absorption bands. Widening is greater on the red side of band.

Tertachlorofluorescein. Shows so slight a shift that it could not be accurately measured. Lowering of temperature causes the appearance and growth of a new band on the red side of the main band.

Sulfonefluorescein. Shows no appreciable shift of the peaks of the main bands as the temperature is lowered, but bands having shorter waves become relatively more prominent.

SPEAS[1] has made a quantitative study of the effect of temperature and concentration upon the absorption bands of some organic solutions. The present paper is a study of the effect of temperature and concentration upon the fluorescence bands of some organic solutions. Use has been made of Speas's paper in comparing the behavior of absorption bands with fluorescence bands.

Experimental

Observations were made by means of a glass spectrograph for temperatures ranging from sixty degrees above zero to sixty degrees below zero or lower. The photographic records thus obtained were compared by means of

[1] W. W. Speas, Phys. Rev. **31**, 569 (1928).

traces made by a microphotometer designed by R. M. Fischer. This microphotometer was modeled after the one described by Perrine.[2] The graphs traced by this apparatus, indicating variations in the density of the photographic negatives, were used to study changes in the intensity of the fluorescence spectra.

Of course these traces do not indicate the actual fluorescence spectra of the substances studied, as the form of the traces depends partly upon the spectral sensitivity of the photographic plate. As the plates are not equally sensitive to all wave-lengths, the photographic records must be a distorted image of the real spectrum. But *changes* in the fluorescence spectrum brought about by raising or lowering the temperature of a solution should be shown more or less faithfully by the photographic records. Traces made by the microphotometer were calibrated and measurements taken from them were used in making graphs for fluorescence bands given in this report.

In all cases, unless otherwise stated, the graphs in a given figure are from a single negative and for equal times of exposure. For this reason the relative heights of the graphs indicate, in a general way, the relative intensities of the fluorescence spectra.

The substances studied were contained either in a rectangular glass cell or in a small glass bottle-shaped cell such as is shown in Fig. 1. The glass cell was closely fitted into a metal chamber *A* surrounded on all four sides and the bottom by an alcohol bath in chamber *B* shown in Fig. 2. A removable tin box was fitted inside *B* so as to fit closely the outside wall of *B*. This box (*C* in Fig. 2) was closed except for an opening *I* to admit liquid air, and one at *O* to allow the escape of the evaporated air. The metal box was fitted into a wooden box for insulation, and the exciting light was admitted through the rectangular opening *L*. The fluorescence light was emitted to the spectrograph through the slit *GD*. The hole *G* in the wooden box fitted closely the end of the collimator of the spectrograph and so shielded the slit from stray light. By having the slit thus guarded from convection currents this housing also prevented the collection of moisture on the slit and on the glass cell. By making the tube *L* extend clear to the outside of the wooden box and then covering the end of the tube by a thin glass window, moisture was prevented from collecting on the face of the cell in front of *L*, and heat from the mercury lamp (which was used as an exciting light) kept the glass window free from moisture.

By admitting liquid air, a drop or two at a time, into *C* the bath could be maintained at any desired temperature below that of the room. When temperatures higher than that of the room were desired, an electric heating coil was substituted for *C*.

In most cases scattered light from the mercury lamp was found to offer very little difficulty in mapping the fluorescence spectra, as the mercury lines, when present, were quite sharply defined and, as a rule, came at parts of the spectrum where their effect could be very easily eliminated when copying the graphs.

[2] J. O. Perrine, J. Opt. Soc. America 8, 381 (1924).

Temperatures were read by means of a pentane thermometer placed so as to press against *A* at *T*.

Rhodamine B was excited by means of an Hanovia quartz lamp. All other plates were made by using a Gallois quartz lamp.[3] This lamp seemed to be about three times as effective as the Hanovia lamp.

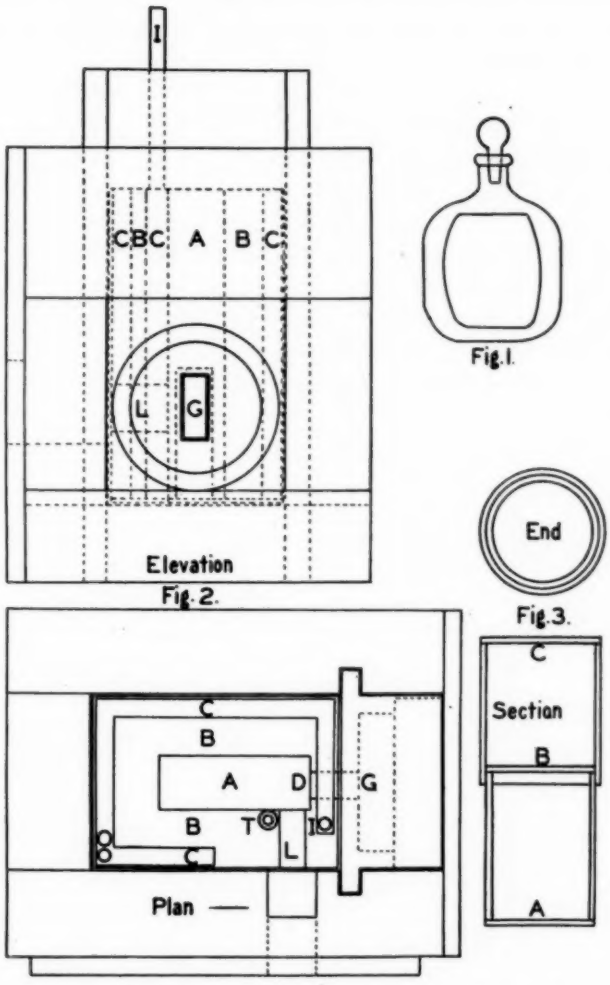

Figs. 1, 2, 3. Diagram of fluorescence cells and mounting.

Because of the wide range of the fluorescence of fluorescein, it was thought best to measure its fluorescence by means of a Lummer-Brodhun spectrometer. Diffused light from an incandescent lamp was used for a comparison source. The same spectrometer was used for measuring absorption.

When measuring absorption, the same container was used that had been used by Speas.[1] But the device shown in Fig. 3 was sub-

[3] M. H. Georg, Revue d'Optique **4**, 89 (1925).

stituted for the device he used for preventing the collection of moisture. It consists of two glass tubes, each about two inches long, partly telescoped. The smaller tube fitted snugly into the metal tube containing the absorption cell, and had a thin glass window over each end. The larger tube fitted snugly over the smaller one and was closed at the outer end by a glass window. A small amount of phosphorus pentoxide was placed in each chamber of this device. This arrangement proved to be quite effective in preventing the collection of moisture.

The solutions were made as needed, and were kept in Pyrex stoppered Pyrex bottles in a dark room. Chemicals were weighed on a chemical balance and dissolved in absolute ethyl alcohol.

Results

Rhodamine B. Solutions were used containing from 0.5 grams per liter to 0.0078 grams per liter. But solutions containing more than 0.0625 grams per liter were so highly absorbant that not enough scattered light from the mercury lamp reached the plate to make it possible to calibrate the traces made from the plates. They were, therefore, not used when making graphs for this report.

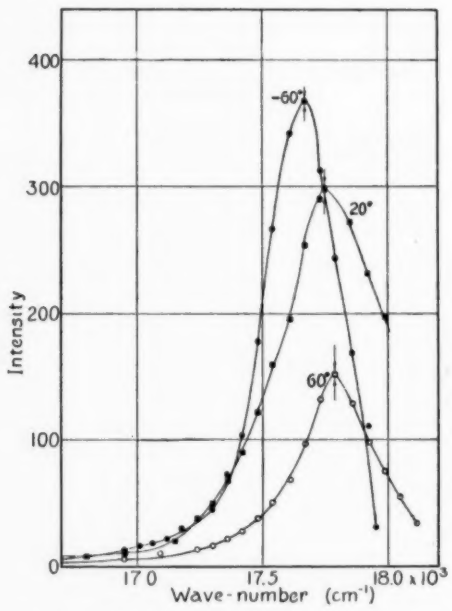

Fig. 4. Fluorescence of rhodamine B. Concentration 0.0625 gm per liter.

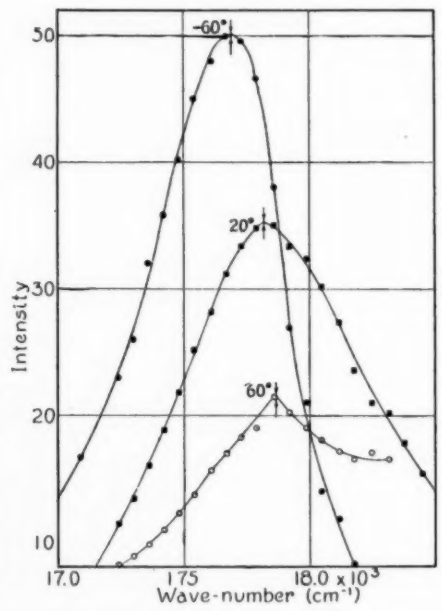

Fig. 5. Fluorescence of rhodamine B. Concentration 0.0156 gm per liter.

The correction factors for the observed values of the fluorescence spectra of rhodamine B are so large that the results obtained are perhaps not very accurate, but they are so consistent that they do doubtless show the nature of the effect caused by change in temperature even if not sufficiently accurate for precise quantitative measurements. Fig. 4 and Fig. 7 are for rhoda-

mine B containing 0.0625 grams per liter. The fluorescence increased steadily as the temperature was lowered. At 60° not enough fluorescence light reached the plate to darken it for concentrations greater than 0.1 grams per liter. For weaker solutions very poorly outlined traces were obtained on the plates, but the photographic records were traced by the microphotometer and an attempt has been made to interpret them.

It will be seen that the fluorescence consists of two bands. The maximum of the stronger band is, at 60°, at about 17,730 cm^{-1}. This band is shown in Fig. 4. The other band is too weak to be shown by the same scale. It is therefore shown in Fig. 7. At 60° this band appears only as a low broad shoulder on the red side of the stronger band. At 20° it is beginning to show a faint maximum which becomes more and more pronounced as the temperature is lowered. The maximum seems to be at about 16,260 cm^{-1} at $-20°$, and at about 16,000 cm^{-1} at $-100°$. The maximum seems to be still further

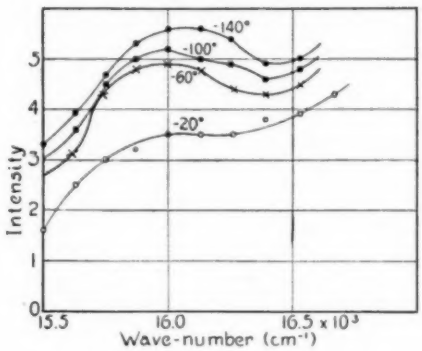

Fig. 6. Fluorescence of rhodamine B. Concentration 0.0156 gm per liter.

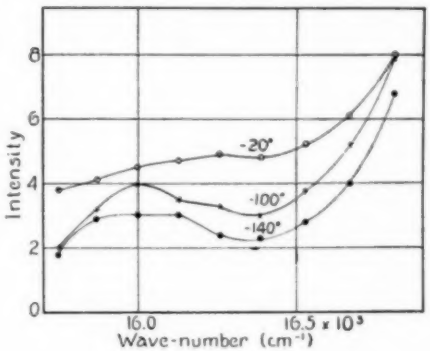

Fig. 7. Fluorescence of rhodamine B. Concentration 0.0625 gm per liter.

toward the red at $-140°$, but the trace in this region for this temperature was irregular near the peak and so the graph is not regarded as reliable. The results shown in Fig. 6 and Fig. 7 are observed values, as absorption does not reach this far toward the red.

Figures 5 and 6 are for a solution whose concentration was 0.0156 gm per liter. The main band is much broader than it was for the stronger solutions. The fluorescence extends farther in both directions as the concentration is lowered and the peak of the band shifts toward longer wave-lengths. The temperature shift is more than it was for the stronger solution by at least twenty percent.

Speas[1] found that the peak of the absorption band shifted to the longer wave-lengths as the solution was weakened. This agrees with the shift found for the peak of the main band of the fluorescence spectrum. The increase in fluorescence of the main band as the temperature is lowered and as the concentration is increased also agrees with the results found by Speas for absorption.

Eosin. The absorption band for eosin overlaps the emission band for such a short distance, and the correction here is so small that it has not

been made except for solutions containing 0.5 gm per liter and for temperatures above $-60°$.

There is an undeniable shift to shorter waves as the temperature is lowered. The shift is apparently proportional to the change in temperature and of the order of 0.6A per degree. Moreover, the temperature shift seems to change very little as the concentration is changed. This may be seen by comparing Fig. 8 and Fig. 9. Fig. 8 is for a concentration of 0.5 gm per liter and Fig. 9 is for 0.02 gm per liter. Lowering the concentration also widens the band as in the case of rhodamine B. The widening is more on the long-wave side of the band.

With both solutions there is a narrowing of the bands as the temperature is lowered. This was also true for rhodamine B. But in the case of eosin

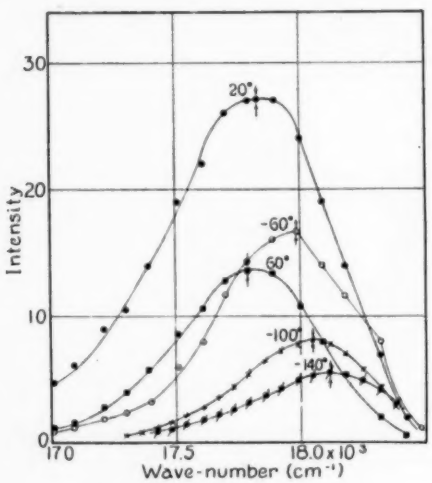

Fig. 8. Fluorescence of eosin. Concentration 0.5 gm per liter.

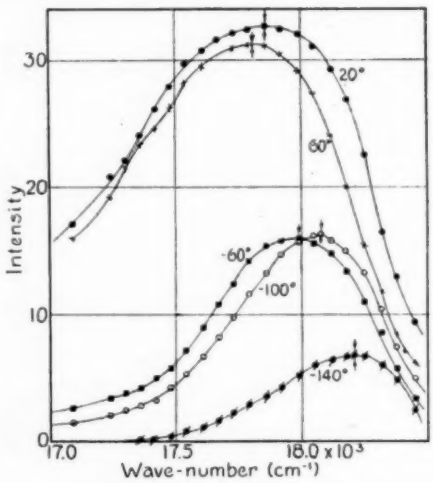

Fig. 9. Fluorescence of eosin. Concentration 0.02 gm per liter.

the fluorescence decreases as the solution is cooled below 20,° which was not the case with rhodamine B.

For both concentrations of eosin the fluorescence was strongest at 20°. The photographic plate indicates that the decrease in intensity between 20° and 60° for the solution containing 0.02 gm per liter is somewhat more than is indicated by the graphs. The intensity for $-100°$ is also less than for $-60°$. The fact that this difference is not shown in the graphs may be due to the fact that it was necessary to change storage batteries which supplied current to the microphotometer lamp while these traces were being made and the current was probably not quite the same for the different traces. Otherwise, the relative intensities for Fig. 9 may have been about the same as for Fig. 8. Speas found no temperature shift for the peaks of the absorption bands and did not try the effect of changing the concentration for neutral eosin.

Fluorescein. The fluorescein solution used was made from a sample of fluorescein recrystallized from acetic acid. As mentioned earlier in this paper,

observations were made by using a spectrophotometer. It was thought best to use the spectrophotometer instead of the spectrograph, as the range of fluorescence was so great that the distorting effect of the plate was quite large when the photographic method was used.

The solution contained 0.5 gm per liter. Measurements were made for temperatures of 60°, 16°, and −55°. The fluorescence was greatest for the the temperature of 16°. Values for the intensity are, of course, relative and not necessarily accurate as the observed intensity must be somewhat affected by stray light from the incandescent lamp which was used as a source of exciting light.

The spectrum seems to consist of two overlapping bands, the weaker band showing as a more or less indistinct shoulder on the short-wave side of the main band. The peak of the main band is at about 19,400 cm^{-1} at 16°. As the temperature is lowered, the peak shifts to shorter wave-lengths.

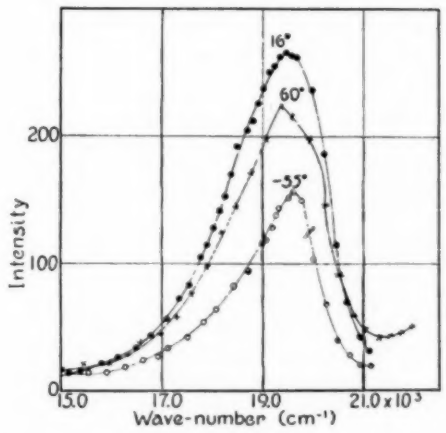

Fig. 10. Fluorescence of fluorescein. Concentration 0.5 gm per liter.

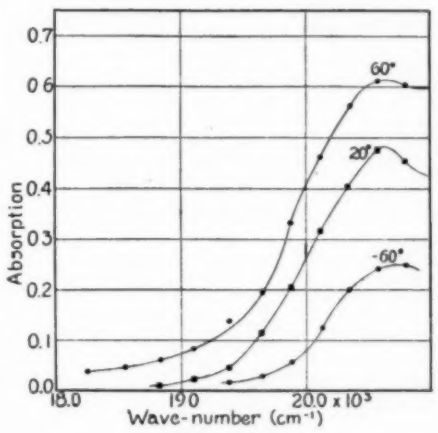

Fig. 11. Absorption of fluorescein. Concentration 0.5 gm per liter.

The shoulder is rather prominent at 60°, but has almost disappeared at −55°. The spectrum reaches from about 16,000 cm^{-1} to beyond 20,800 cm^{-1} and fades more rapidly on the short-wave side than it does on the other as the temperature is lowered.

The coefficients of absorption were measured but were found to differ only slightly from the values found by Speas for samples used last year. There is very little, if any, shift in the peaks of the absorption bands.

Tetrachlorofluorescein. The fluorescence curve for tetrachlorofluorescein is shown in Fig. 12. The solution contained 0.4 gm per liter. The absorption band overlaps the emission band for so short a distance that no correction for absorption is necessary when plotting the fluorescence. Whether there is a shift in the peak of the fluorescence band cannot be definitely determined It is true that the peaks as shown by the graphs in Fig. 12 indicate a probable shift, but in order to get a plate sufficiently dense it was necessary to use

so wide a slit and such a long exposure that the mercury lines which were used for calibration were so broad that it was hard to tell just what part of their traces should be used as reference lines for calibration.

At room temperature (20°) there seems to be but one band and this is steeper on the red side than on the violet side. In this respect it differs from any other substance studied. The fluorescence is also very much stronger at $-20°$ than at 20° and does not change much in intensity below this temperature until the solution is cooled below $-100°$. Below $-100°$ the fluorescence begins to fade and at $-140°$ the fluorescence is so weak as to be entirely masked by scattered light from the mercury lamp. No good traces were obtained for temperatures above 20° or below $-100°$.

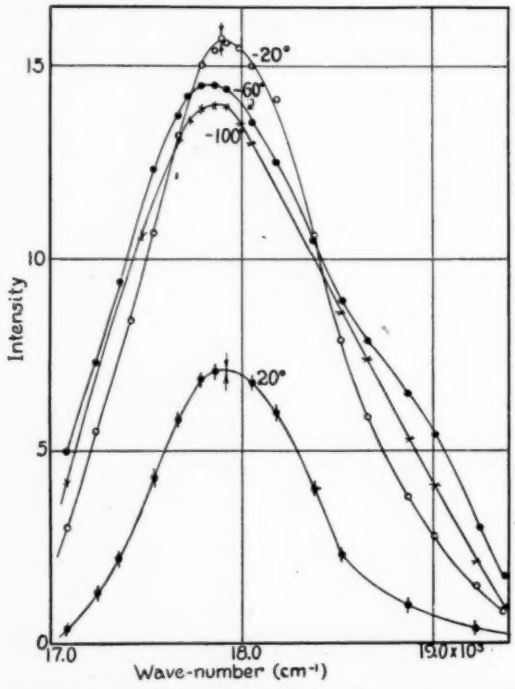

Fig. 12. Fluorescence of tetrachlorofluorescein. Concentration 0.4 gm per liter.

Unlike most of the substances studied, there is very little change in the width of the band as the temperature is lowered.

Sulfonefluorescein. The graphs in Fig. 13 show the results obtained for sulfonefluorescein. The fluorescence spectrum extends from 16,500 cm^{-1} to 20,900 cm^{-1}. As the sensitivity of the plate varies decidedly from place to place in this region, the actual spectrum must differ widely from that indicated by the graph. The photographic plate was most sensitive for wave-lengths greater than 5500A so that this end of the spectrum appears relatively too intense. The sensitivity of the plate decreased for waves shorter than 5600A until minimum sensitivity was reached for waves whose lengths were about 5200A. It then slowly increased until a wave-length of about 4650A

was reached and then slowly decreased again. It will be seen, therefore, that the middle part of the spectrum is decreased in brightness and that both ends appear relatively more intense than they should. However, it seems probable that three peaks do actually occur. It is certainly true that the short-wave side of the spectrum increases in relative prominence and that the long-wave side decreases as the temperature is lowered. None of the peaks seem to shift with change in temperature. It seems probable that the center band is strongest at room temperature, that the long-wave band

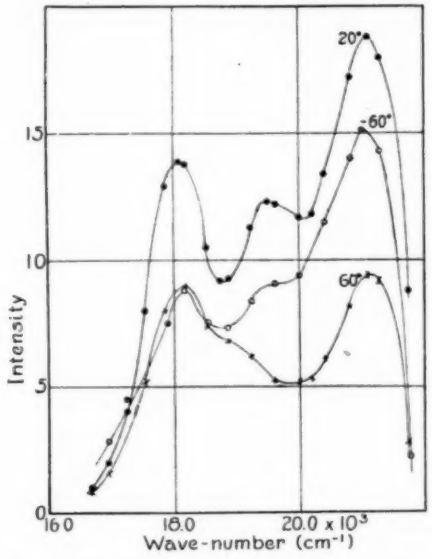

Fig. 13. Fluorescence of sulfonefluorescein.

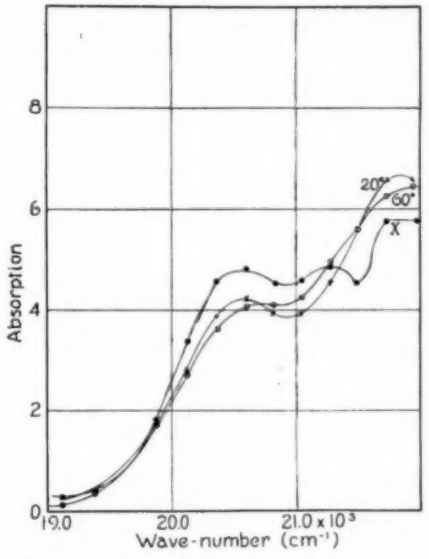

Fig. 14. Absorption of sulfonefluorescein.

decreases and that the short-wave band increases continuously as the temperature is lowered. There is no apparent shift in the position of the absorption bands with change in temperature. The graphs for the absorption bands are given in Fig. 14. The temperature marked *X* was not accurately determined. The thermometer was broken before this run was completed and another could not be found to replace it. It was intended that the temperature should be $-60°$, but it was probably somewhat lower than this for the latter part of the run.

Discussion

The many striking analogies between the behavior of the absorption spectra and that of the fluorescence spectra of the different substances studied suggest that they both obey very similar laws. In his report on the effect of temperature upon the absorption spectra, Speas gives graphs for rhodamine B for concentrations of 0.004 gm per liter, 0.160 gm per liter, and 0.5 gm per liter. Graphs are given for temperatures of 60°, 17°, and $-68°$, for solutions containing 0.5 gm per liter; for temperatures of 60°, 18°, and $-65°$ for solutions containing 0.160 gm per liter; and for temperatures of 60°

18°, −65° and −90° for solutions containing 0.004 gm per liter. Using Speas' data, graphs have been plotted for a given temperature using wave-numbers in cm^{-1} for the peak of the absorption band as abscissae and logarithm of the concentration as ordinates. As shown in Fig. 15, straight lines intersecting at a common point represent the data fairly well. Then, using corresponding wave-numbers as abscissae, but plotting temperatures as ordinates for a given concentration, straight lines were obtained. Apparently the lines showing the temperature shift also meet at a point. It is remarkable that the abscissa of this intersection point is the same for the temperature shift as it is for the concentration shift. But perhaps this should have been expected. For, since the concentration shift decreases as the temp-

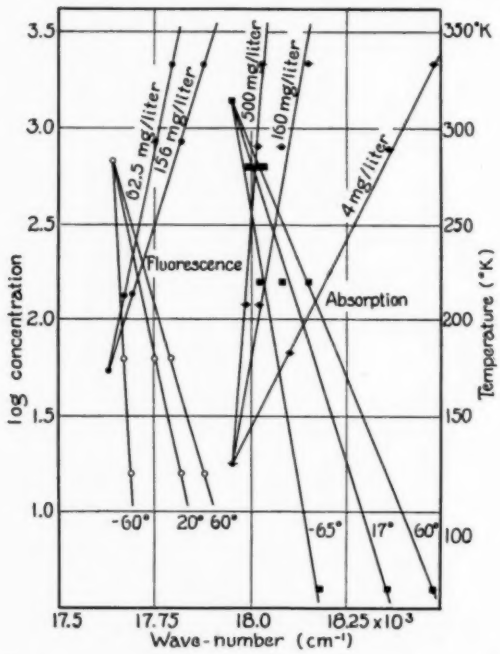

Fig. 15. Variation with concentration and with temperature of the peaks of the fluorescence and absorption bands of rhodamine B.

erature decreases, there should be some temperature for which the position of the peak is constant for all concentrations. Call this peak ν_c. Also, since the temperature shift becomes less as the concentration is increased, there should be some concentration for which the position of the peak is the same for all temperatures. But this solution may have the particular temperature for which the peak of the band is ν_c. Therefore, the graph for zero temperature shift should coincide with the graph for zero concentration shift.

Assuming that the same law holds for the fluorescence spectrum as for the absorption spectrum, it was found that straight lines could be drawn through the points representing the position of the peaks of the fluorescence spectrum of rhodamine B that would meet at a critical concentration for

zero shift as for the absorption bands. This located the peak of the fluorescence band for the critical concentration at about 17,630 or 17,640 cm^{-1}. It was also found that lines for the temperature shift might be drawn through this same peak. This is shown in Fig. 15.

Fig. 16 shows the temperature shift for rhodamine B, eosin, and fluorescein. These two sets of graphs (Fig. 15 and Fig. 16) seem to show that the concentration shift is proportional to the change in the logarithm of the concentration and that the temperature shift is proportional to the change in

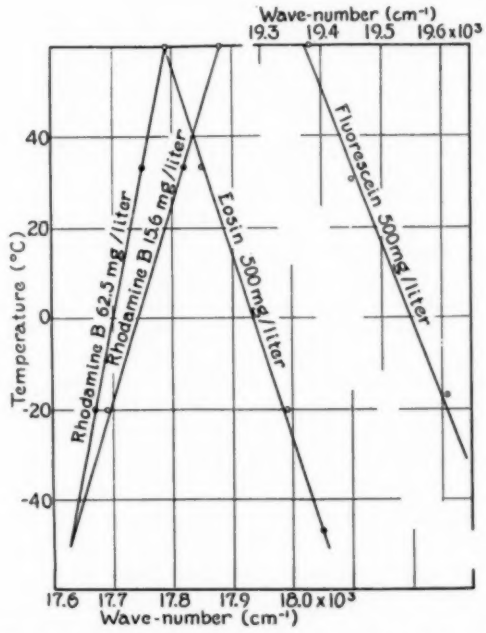

Fig. 16. Variation with temperature of the peaks of the fluorescence bands of rhodamine B, eosin and fluorescein.

temperature. The temperature shift is not the same for all solutions, but for a given substance it is always in the same direction for fluorescence as that found by Speas for absorption. Fig. 15 also shows that the concentration shift and the temperature shift for fluorescence obey the same law as the corresponding shift for absorption.

I wish to express my gratitude to Professors Gibbs and Merritt for suggesting this topic, to Professor Gibbs for criticism and suggestions while the work was being done, and to Dr. Shapiro for supplying me with chemicals.

LETTERS TO THE EDITOR

Prompt publication of brief reports of important discoveries in physics may be secured by addressing them to this department. Closing dates for this department are, for the first issue of the month, the twenty-eighth of the preceding month; for the second issue, the thirteenth of the month. The Board of Editors does not hold itself responsible for the opinions expressed by the correspondents.

Alternating Intensities in the Absorption Bands of Li_2

The absorption spectrum of lithium vapor shows two band systems in the visible, one in the red and another in the blue-green. Both in position and structure they are strikingly similar to the corresponding bands of Na_2, which have been studied in detail. We expect, however, two interesting features not shown in Na_2. The bands of the isotopic molecule Li^6Li^7 should have about 1/15 the intensity of the stronger Li^7Li^7 bands, and hence should be observed. Furthermore, the rotational structure of the bands due to the symmetrical molecule Li^7Li^7 should show alternating intensities unless the nuclear spin is too large, as it appears to be in Na_2. We have undertaken a study of the structure of the two Li_2 band systems, and have been able to confirm the existence of alternating intensities in the lines of the blue-green system. Detection of the isotope effect will require a modification of our experimental conditions.

From our preliminary results, the heads of the blue-green system are given approximately by

$$\nu = 20{,}398.9 + 268.0n' - 3.24n'^2 - 349.0n'' + 2.66n''^2.$$

The vibrational intensity distribution is very similar to that in the corresponding system in Na_2, which is to be expected since the ratio of the vibration frequencies in the lower and upper states, ω_0''/ω_0', is nearly the same in the two cases (1.30 for Li_2; 1.27 for Na_2). It therefore seems possible that the blue-green systems of these two molecules are due to the same type of electronic transition, $^1P \rightarrow {}^1S$. A preliminary study which has been made of the rotational structure of the (0, 0) band, λ4901, using the first order of a 15-foot concave grating, confirms this view, since three branches are found, of which the Q is the strongest.

The alternation of intensity in successive lines of a given branch is very apparent on microphotometer curves taken with the new Zeiss instrument in this laboratory. Thus the electrometer deflection for every other line in the P and Q branches (some 52 lines in all) is without exception smaller than the mean deflection for the two adjacent lines of the same branch. The same alternation is observed in the case of the R branch, but here the branch is rather weak and the irregularities consequently more pronounced. The average ratio of the electrometer throws for adjacent lines is 1.19:1 for the Q branch and 1.24:1 for the P and R branches (mean value for the two). In order to estimate the alternation factor for intensities from the microphotometer readings, we may assume the law of blackening $S = a + \gamma \log I$. The calculations show that, with any reasonable value of γ for the plates used, the alternation ratio cannot exceed 1.33:1 and more probably is in the neighborhood of 1.20:1. The latter value would require an unexpectedly large value for the nuclear spin, 5 Bohr units. This result may be significant, however, since hitherto it has been impossible to account for certain satellites of wide separation in the hyperfine structure of the atomic Li lines by referring them to nuclear spin. In the quantitative intensity measurements to be carried out later, statistical methods will have to be adopted, because of the numerous irregularities in the intensities due to blending with lines of faint underlying bands, etc.

A. HARVEY
F. A. JENKINS

Department of Physics,
University of California,
October 18, 1929.

A Photoelectric Cell for use in Erythema

The curve for the absolute sensitivity of a lithium photoelectric cell in quartz (non-sensitized, vacuum type) has a maximum at 2800A, in the spectral region most effective for some biological work. The sensitivity is of the same order of magnitude as that of the most sensitive Kunz type gas-filled sodium or potassium hydride cells.

With a filter (one cm thickness of a 50 percent aqueous solution of nickel sulphate[1] with 6.38 mm of Corning glass G985B) the maximum of the curve for lithium is shifted to 3000A, which is very near the maximum of the erythema curve.[2] The maximum point of a similar cadmium cell, which has been suggested for use as an actinometer, is at a wave-length less than 2500A, while at 2800A and at 3000A the lithium cell is over 600 times as sensitive as the cadmium cell.

F. W. Cook

Physics Laboratory,
University of Illinois
October 25, 1929.

[1] Jones, J.O.S.A.&R.S.I. **16,** 259(1928).
[2] Hausser and Vahle, Strahlentherapie **13,** 41(1921–1922).

Electron Diffraction by a Copper Crystal

The diffraction of electrons by a single crystal of copper has recently been investigated by H. E. Farnsworth.[1] With but two exceptions, he observed all of the expected electron diffraction beams that are the x-ray analogues in the region studied. Twelve space lattice beams were found that require a double crystal spacing or a wave of one-half the length given by $\lambda = h/mv$. Eight of these beams are in the (100) azimuth and four are in the (111) azimuth. Farnsworth pointed out that since most of these beams are in the (100) azimuth they must arise from the structure of the crystal. Eight additional beams were not accounted for by either of the above methods. Seven of these were of low intensity and broad appearance; one was quite strong.

For a copper crystal (face-centered cubic) and a wave-length given by $\lambda = h/mv$, one expects space lattice diffraction beams corresponding to the intersections of solid lines and solid curves in Farnsworth's two diagrams; for a wave-length given by $\lambda = h/2mv$ one expects beams corresponding to all intersections in both diagrams. If the crystal was simple cubic with the dimensions of the face-centered structure then one would expect diffraction beams corresponding to all intersections in the (100) diagram, but only to intersections of dotted and solid curves with solid lines in the (111) diagram. This last case gives the most complete and accurate description of Farnsworth's results. It includes the assumption that electron beams arising from planes not having all indices odd in odd orders are not completely suppressed.

If the correlation is accepted as an accurate one, then reflection from other possible crystal planes, such as (521), might be expected if the examination should be made in the correct azimuth. Some of the additional beams observed by Farnsworth that do not correspond to intersections of curves and lines on the diagrams might be of this type, since due to the relatively poor, as compared with x-rays, resolving power of his apparatus some plane reflecting in an azimuth but slightly displaced from (111) or (100) azimuth might still give a beam appearing in one of these. The low intensity of some of these extra beams might be due to their being examined at some voltage and angle other than the ones leading to their maximum development.

R. Ironside[2] has recently investigated the diffraction of high velocity electron beams (29 to 62 KV) from thin copper films. He found only those diffracted beams analogous to x-ray diffracted beams from a face centered lattice. It thus seems that the phenomena observed by Farnsworth are partially to be explained by the small penetration of low velocity electrons (10–300V) below the surface of the crystal. The experiments of Farnsworth are at variance with those of Davisson and Germer.[3] This disagreement

[1] H. E. Farnsworth, Phys. Rev. **34,** 679 (1929).
[2] R. Ironside, Proc. Roy. Soc. **A119,** 668 (1928).
[3] Davisson and Germer, Phys. Rev. **30,** 705 (1928).

might be explained in a phenomenological manner, the (100) face of a copper crystal was used in the former case while the (111) face of a nickel crystal was used in the latter. The explanation might be found in the difference in background scattering and resolving power in the two cases; the additional beams observed by Farnsworth were relatively weak. It seems rather that a true discrepancy is apparent here.

In conclusion it might be mentioned that a few cases are known in the reflection of x-rays from crystals in which forbidden (by the usual treatment of interference) orders of reflection from a plane are present; for example (111) 2nd order from diamond and (111) 1st and 3rd orders from rubidium bromide using strontium K radiation.

STERLING B. HENDRICKS

Bureau of Chemistry and Soils,
Washington, D. C.

Reflection of Lithium Ions from Metal Surfaces

In some experiments similar to those of Read (Phys. Rev. **31,** 155, 1928) and of Gurney (Phys. Rev. **32,** 467, 1928) on the reflection of positive ions from metal surfaces, the writer has discovered what appears to be a fairly well defined beam of reflected lithium ions which retain a large fraction of their energy of impact. This beam, when present, occurred in addition to the approximately specular reflection found by Read and Gurney, in which most of the ions lose a considerable part of their original energy.

Two reflectors were used, one of platinum foil and one of nickel crystals deposited on a tungsten foil by evaporation, according to the method of Rupp (Ann. d. Physik **1,** 801, 1929). With this method the nickel crystals are formed with the (111) planes parallel to the surface of the tungsten foil.

The angle at which the new reflected beam appeared was observed for several angles of incidence. Observations were made in the plane containing the incident beam and the normal to the reflector. With the nickel crystal reflector, a beam making an angle of 21° with the surface gave a reflected beam making an angle of 81° with the surface. For grazing angles of 27.5° and 39° reflected beams at 84.5° and 82° were observed, while with 48° (angle of incidence 42°) the beam was not found. With the platinum reflector an incident beam making an angle of 31° with the surface gave a reflected beam at 88° with the surface, while with a grazing angle of 46° no reflected beam was observed.

The new beam did not appear with low velocity ions, but appeared when accelerating potentials between 200 and 250 volts were used and continued *without change in angle* up to 700 volts, the highest voltage used. The beam could not be detected until retarding voltages had been applied to suppress some of the general reflection of low velocity ions described by Read and Gurney. With retarding potentials of 10 percent of the accelerating potential the beam was noticeable. Most of the ions in the beam retained 80 percent or more of their original energy.

A provisional explanation of the angles observed with the nickel reflector is that the ions are specularly reflected from the (110) planes in the nickel crystals. This gives an angle for the reflected beam that agrees approximately for two of the three angles observed.

R. B. SAWYER

Ryerson Physical Laboratory,
University of Chicago,
October 24, 1929.

A Theoretical Interpretation of Hyperfine structure

At the present time the most satisfactory explanation of the hyperfine structure in spectral terms and lines is obtained by assigning an angular momentum to the nucleus, or to part of the nucleus, of an atom. Sufficient data are now available on hyperfine structure to indicate that the widest fine structure term separations are to be expected for those terms arising from electron configurations involving a single s electron. This is to be expected since an s electron is found part of the time near to the nucleus and part of the time outside of all the other electrons. Fine-structure observations indicate that a deep penetrating electron merely serves to strengthen the coupling between nucleur angular momentum i and the electron resultant J. This leads to

the postulate that *for multiplet terms which show LS coupling, and for which there is but one deeply penetrating s valence electron involved, (a) the total fine-structure separations for each term should be given by cos Si when cos Ji=1 and J≧i; and at the same time (b) the relative separations of fine-structure for each term should be given by cos Ji. When cos Si is positive the fine-structure terms should be normal, when negative they should be inverted. For a positively charged nucleur spin the reverse is true.* When more than one valence electron is quite deeply penetrating, the vector sum of the separate electron couplings with i determines the total fine-structure separations. Excellent confirmations of the above theoretical interpretations have been found in the spectra of Bi I, Cd I, Tl I, Tl II, Ba I, Mn I, La I and La II. The inversion of fine structures, and apparent sharpness for other terms, within a given multiplet term is found in the $^3D6s7d$ terms of Tl II, the ^3D and ^1D $6s5d$ terms of La II, the ^3P and ^1P $6s6p$ terms of Tl II, the ^2D $6p^2$ terms of Bi I, and the ^4F $5s5d^2$ terms of La I. The role played by a single s electron is beautifully displayed in the first three members of the series $^3S_1$ $5sms(m=6,7,—)$ terms of Cd I where the separations in cm^{-1} are 0.397, 0.375, and 0.364 respectively. Here the limit obviously is $^2S_{\frac{1}{2}}5s$ with doublet fine-structure separation about 0.350 cm^{-1}. Two members of two such series are also found in Tl II, ^3P $6smp(m=6,7,—)$ and ^3D $6smd$ $(m=6,7,—)$ of which the $^2S_{\frac{1}{2}}6s$ limit must have a fine-structure separation of from 3 to 4 frequency numbers. A more detailed explanation is forthcoming in a succeeding number of the Physical Review.

H. E. WHITE

Physikalisch-Technische
Reichsanstalt
October 19, 1929.

Indetermination Principles Involving k and e

Continuing the study of the symbolical equivalence of physical concepts and relations (J.Q. Stewart, Physical Review **33,** 637, 641; **34,** 1052, (1929), the following schedule of equivalent "dimensions" in tentatively proposed.

1. *Heat*	2. *Electricity*	3. *Mechanics*
A Entropy	Charge	Action
B Temperature	Potential	Frequency
C Volume	Area	Distance

By reference to this vocabulary an equation or definition in mechanics may be translated into an equation or definition in either heat or electricity, and conversely. For example, *momentum* being action divided by distance, the equivalent electrical concept is *field*, which, dimensionally, is charge divided by area; and the equivalent concept in heat is *entropy per unit volume. Velocity*, on the other hand, with dimensions *BC*, corresponds to *potential multiplied by area*, and to *temperature multiplied by volume.* Whether these quantities can be given significance remains to be seen. Obviously the detailed application in physics of this system will involve much study.

As previously suggested, Boltzmann's constant k, "Millikan's constant" e, and Planck's constant h, are symbolically equivalent. In addition to the famous group of indetermination equations containing h, based on

$$\Delta p \cdot \Delta q > h,$$

where Δp is uncertainty in momentum-Δq in coordinate—indetermination princie ples should exist involving k and e in plac, of h.

The following rough argument indicates that k does enter in an indetermination equation,

$$\Delta\sigma\Delta v = k, \qquad (1)$$

where Δv is uncertainty in volume, and $\Delta\sigma$ is uncertainty in entropy, per unit volume. For, consider the well-known fluctuations in volume v of a perfect gas, containing N molecules, and forming part of a much larger volume. The entropy is Nk log vT^{α} plus a constant, and the change in entropy due to a change Δv in volume, T(temperature) being constant, is $Nk\Delta v/v$, or $Nk\Delta v/v^2$ per unit volume. (When the change Δv is associated with a "fluctuation," instead of with a slow change, in thermodynamic equilibrium, this result is in doubt, however.) Substitution in (1) gives

$$\Delta v = v/N^{\frac{1}{2}}$$

But $v/N^{\frac{1}{2}}$ is exactly the expected fluctuation in v, as found in kinetic theory—and (1) is confirmed.

The corresponding indetermination principle involving e is

$$\Delta F \Delta s = \beta e \qquad (2)$$

where ΔF is uncertainty in electric field and Δs is uncertainty in area, while β is some pure number not greatly different from unity. It is to be noted that the equation

$$\int F ds = 4\pi n e,$$

when the integral is over any closed surface, and n is integral, expresses Gauss's theorem and the "quantization" of electric charge—just as the integration through a cycle,

$$\int p dq = nh,$$

introduces the quantization of action.

The experimental test of (2) may be possible in a variety of ways. The following method appears promising, although it involves additional assumptions and might fail even though (2) were correct. Suppose electromagnetic radiation is passing from a point source, at distance r, across an area s. Interpret ΔF as the mean amplitude of the electric vector of the radiation. If the light is very feeble, (2) implies, then, that Δs is relatively large. The question therefore arises: can a distinct image of a small area be formed with very faint light? This is a variation of the old problem of whether interference persists with faint radiation.

Numerical calculations, based on an extension of this argument, indicate that it may be possible photographically to detect such an effect. An experimental test is in progress, conducted by the writer and Mr. S. A. Korff.

JOHN Q. STEWART

Princeton University
October 24, 1929.

BOOK REVIEWS

Verstärkermesstechnik. MANFRED VON ARDENNE. Pp. 232, figs. 246. Julius Springer, Berlin, 1929. Price, bound, RM 24.

This book aims to give a critical digest of the literature on *the techinque of amplification measurements* from about 1923 to 1928. The contents comprise: Instruments, Methods, Source of Error, Bibliography. The emphasis is placed on the practical rather than on the theoretical aspects. The treatment is quite thorough. The sentence structure is at times involved, making the reading difficult. The printing and illustrations are good but the finish and binding are "cheap." J. A. BECKER

Introduction to College Physics. C. M. KILBY. Pp. 341, 349 figs. D. Van Nostrand Company, New York. Price $3.00.

In many introductory courses in college physics, time is not available to do justice to the average text of from 600 to 700 pages, and a more concise text is required. The above book of 341 pages was planned to meet such a need. Brevity has been obtained by a certain amount of topical selection which covers the ground fairly well from a conservative standpoint. Only the most fundamental illustrations are used, thus leaving opportunity for amplification by the instructor in the class room. Probably the greatest reduction has been obtained by brevity of statement. Photographs are omitted, simple diagrams being employed throughout. A full list of straightforward problems is included.

The author has set himself a very difficult task with only moderate success. One is disappointed to find that due to the extreme brevity of statement the reader is frequently led to make wrong inferences. Use is made of terminology and conceptions which are not explained to the student. This is not so much noticed by one familiar with physics, but to the young student it is a source of real difficulty. Also it is very unfortunate that errors of classification and statement of fact have been allowed to creep in. Some illustrations are given below.

Count Rumford . . . . showed that heat can do work." Illustrating forced vibrations: "If a pendulum with an iron bob vibrates over a strong magnet, its period will be different from its natural period." "Shumann [sic] waves . . . . $1.3\times10^{-6}-4.5\times10^{-7}$ cm." "At different temperatures . . . . the calorie is somewhat variable . . . . ." "Snow appears white because the light on it is reflected from the internal faces of the crystals." Illustrating thermal expansion of different substances: "A piece of celluloid placed in the palm of the hand will buckle because one side is heated more than the other," (neglects effect of moisture of hand); "The breaking of a thick glass bottle . . . . ." "It is not easy to understand how energy in the form of waves can be radiated and absorbed by an oscillating electrical charge (electron). These new difficulties have been met in part by the quantum theory . . . . ."

In view of the real need of an accurate, concise text with a good selection of topics from the standpoint of modern physics, one is disappointed to find such handicaps in the above text. R. C. WILLIAMSON

Fundamentals of Physics. A. L. FITCH. Pp. 336, figs. 100. Thomas Y. Crowell Company, 1929. Price $2.50.

Every teacher of general physics is much perplexed with the large number of topics which seem worth while, indeed are necessary, to include in a year's course. The subject itself is growing rapidly in these days of such unparalleled activity in physical research and speculation, but the capacity of our students to assimilate facts and principles seems to remain about constant. This book is the result of one teacher's effort to trim and cut the material to fit the time allotted. Probably many teachers will not agree with the author's choice of what to omit, but we shall have to admit that he has dared to make a short textbook.

The author frankly faces the fact that physics requires some mathematics for its mastery and has generously sprinkled his text with algebraic proofs of the fundamental equations. In fact, he has included a bit of the nomenclature of the calculus. It might be well for the teachers who use this text to omit from their lectures such demonstrations on the blackboard and devote the time thus saved to experimental demonstrations. Surely this would meet with the approval of the students. The author has recognized the historical development of the science by including eighteen full page portraits together with excellent biographical notes.

The book is written in a very concise style, which is doubtless clear to the instructor but will not always seem so to the student. Sometimes valuable space could have been saved by reducing the scale of the diagrams and adding more labels so that each diagram would tell its own story. It would also have been helpful to number the cuts and refer to them specifically in the text. Teachers will welcome the list of 156 supplementary problems at the end of the book.

N. HENRY BLACK